NPL REPORT CETM 46

REPORT

CCEM KEY COMPARISON CCEM.RF-K3.F (GT-RF 92-1)

Measurement Techniques and Results of an Intercomparison of Horn Antenna Gain in IEC-R 320 at Frequencies of 26.5, 33.0 and 40.0 GHz

D G Gentle, A Beardmore, J Achkar,
J Park, K MacReynolds & J P M de Vreede.

September 2003

NPL
National Physical Laboratory

NPL Report CETM 46, September 2003

CCEM KEY COMPARISON CCEM.RF-K3.F (GT-RF 92-1)

Measurement Techniques and Results of an Intercomparison of Horn Antenna Gain in IEC-R 320 at Frequencies of 26.5, 33.0 and 40.0 GHz.

by

D G Gentle and A Beardmore (NPL),
Dr J Achkar (BNM-LCIE),
Dr J Park (KRISS),
K MacReynolds (NIST),
Dr J P M de Vreede (NMi-VSL)

Edited and assembled by D G Gentle (NPL)
Centre for Electromagnetic and Time Metrology
National Physical Laboratory (NPL)
Teddington, Middlesex, TW11 0LW

ABSTRACT

A measurement comparison of the boresight gain of two IEC-R320 horn antennas has been carried out between five national metrology laboratories at 26.5, 33 and 40 GHz. The following five national metrology laboratories participated: NPL (United Kingdom), NMi-VSL (The Netherlands), NIST (United States of America), BNM-LCIE (France) and KRISS (Republic of Korea). The National Physical Laboratory (United Kingdom) acted as the pilot laboratory for the comparison.

ISSN 1467-3932

National Physical Laboratory
Queens Road, Teddington, Middlesex, UK, TW11 0LW

Approved on behalf of the Managing Director, National Physical Laboratory by
Dr S Pollitt, Head of the Centre for Electromagnetic and Time Metrology

Contents

1. INTRODUCTION

The CCEM international antenna gain comparison CCEM.RF-K3.F was initiated by the Working Group on Radio Frequency quantities (GT-RF) of the Consultative Committee for Electricity and Magnetism under reference GT-RF 92-1. The purpose of the comparison was to evaluate the consistency between the participating laboratories in the measurement of the boresight gain of horn antennas in IEC-R320 (EIA WR-28 or British WG22).

Two commercially produced pyramidal horn antennas were selected for the comparison, one with a nominal mid-band gain of 16.5 dB and the other 24.3 dB.

The current comparison is a follow on from the comparison GT-RF/78-5, which was carried out in IEC-R100 (EIA WR-90 or British WG16) and piloted by NIST.

2. PARTICIPANTS.

David Gentle / Andrew Beardmore
National Physical Laboratory **(NPL)**
Teddington TW11 0LW.
United Kingdom

Jan de Vreede
Nederlands Meetinstituut -Van Swinden Laboratorium **(NMi-VSL)**
Schoemakerstraat 97
2628 VK Delft
The Netherlands

Katie MacReynolds / Jeff Guerrieri
National Institute of Standards and Technology **(NIST)**
Boulder, Colorado 80303-3328.
USA

Jeongil Park
Korea Research Institute of Standards and Science **(KRISS)**
PO Box 102
Yusong, Taejon 305-600
Republic of Korea

Joseph Achkar / Laurent Velasco
Laboratoire Central des Industries Electriques **(BNM-LCIE)**
33 Avenue du Général Leclerc
92260 Fontenay-aux-Roses, Cedex.
France

3. TRAVELLING STANDARDS

Two comparison standards were used:

1) A Narda model V637, with nominal mid-band gain of 16.5 dB marked “INT” and “9411”.

2) A Scientific Atlanta (SA) model 12A-26, with nominal mid-band gain of 24.3 dB, serial number 16056HC, marked “INT”.

An additional Narda model V637 antenna was also provided for those participants wishing to use a three antenna technique, but not possessing the third antenna.

The dimensions of the antennas are given below:

Nominal Antenna Dimensions

Horn	A [mm]	B [mm]	C [mm]
Narda V637	44	26	20
SA 12A-26	177	71	59

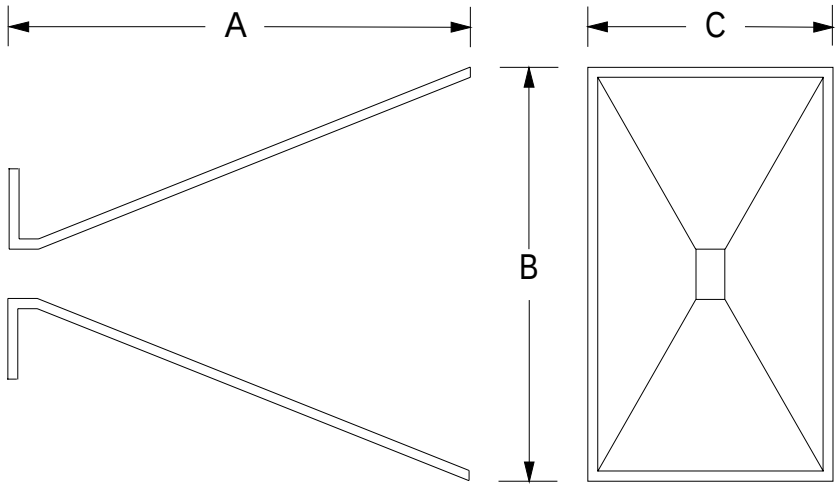

Figure 1: Dimensions of the travelling standards.

The particular comparison standards were chosen because of their differing designs and gains. The walls of the flared section of the Narda antenna are curved, whereas those of the Scientific Atlanta antenna are flat. The gain of the Narda antenna is low enough that the far-field distance can be realised in an anechoic chamber of moderate size, whereas that of the Scientific Atlanta horn is much greater and some form of near-zone correction would be required to get the true far-field gain.

4. PARAMETERS FOR MEASUREMENT

The comparison protocol requested the following parameters to be measured:

Gain

The boresight gain was requested at 26.5, 33.0 and 40.0 GHz for both antennas. The boresight line was defined as the normal to the input flange of the antenna, not the normal to the aperture. This definition was used because the aperture edges of these antennas do not generally lie in a plane, this being particularly true of the Scientific Atlanta antenna.

Reflection Coefficients

The real and imaginary parts of the reflection coefficients of the antennas.

Swept Frequency Measurements

As an option, participants were invited to perform swept frequency measurements of the gain over the frequency range 26.5 GHz to 40.0 GHz.

5. THE COMPARISON SCHEDULE

The travelling standards were circulated to the participating laboratories in the following order:

NPL (UK)	October/November 1998
NMi-VSL (Netherlands)	May 1999
NIST (USA)	August 1999
BNM-LCIE (France)	September/October 1999
NPL (UK)	December 1999
KRISS (Korea)	February/March 2000

6. METHODS OF MEASUREMENT

NPL (1) & NPL (2)

The gains of the antennas were measured by the three antenna extrapolation technique in an anechoic chamber measuring: 10.7 m x 5.3 m x 4.3 m (L x W x H) and lined with 0.61 m RAM [1]. The transmitting and receiving antennas were aligned by auto-reflection using a micro-alignment telescope with a parallel sided mirror mounted on the flange of the waveguide. Thus the gain was measured

along an axis normal to the input flange of the antenna. To reduce the effect of bending under the weight of the antenna, the sections of waveguide used to support the antennas were specially constructed for the purpose from flange stock and were therefore thick walled and stiff.

The antennas used in the three antenna technique were the two comparison antennas plus a second Narda model V637 horn that had been calibrated at NPL many times previously. The insertion loss was measured for antenna separations ranging from 20 cm to 80 cm for measurements involving the two Narda antennas and from 110 cm to 300 cm for those in which the Scientific Atlanta antenna was used. The separations were measured by a laser interferometer system and a low pass filter was included in the transmitting circuit to reduce source harmonics. A thermistor sensor based power measurement system was employed with one sensor connected to the side arm of a high directivity directional coupler in the transmitting circuit and a second one connected to the end of the receiving waveguide section.

Prior to fitting the data was digitally filtered to remove the effect of multiple reflections between the antennas. For the extrapolation data processing, a three term fit was used with a maximum to minimum distance ratio of 2.7.

A Hewlett-Packard 8510C automatic network analyser was used to measure the complex reflection coefficients of the antennas and other components used in the measurement circuit. Mismatch corrections were calculated using these measured reflection coefficients and applied to the measured gains to give the true gain of the antennas according to the IEEE definition of gain.

During the first set of measurements made at NPL, the gain and reflection coefficients were measured from 26.5 GHz to 40 GHz in 250 MHz steps to provide stepped, swept frequency coverage. When the antennas were remeasured in December 1999, the measurements were performed at 26.5, 33.0 and 40.0 GHz only.

A three antenna measurement was also made at a fixed distance of 4.5 m both with the thermistor based power measurement system and also one using diode power sensors. These measurements were used to aid the identification of systematic errors, as the gain of the Narda horn measured at 4.5 m will be close to its far-field value.

All measurements were performed at (23 ±2)°C.

NMi-VSL

The measurements were done using a renovated semi-anechoic room (i.e. the side from which the transmitter is emitting is open). A three-antenna method was used. Aside from the two horns to be investigated an additional horn, supplied by the pilot laboratory, was used most of the time, and in some other cases a VSL-owned horn.

Transmission measurements have been performed for different separations between transmitter and receiver, however only those performed at the largest separation (about 4.2 m) were used in the final analysis. No extrapolation or near-zone corrections have been applied to the results.

Two different combinations of three horns were used during the investigation of the two DUTs:

1) A set containing the two DUTs and a VSL-owned horn of Flann (standard gain horn)
2) A set containing the three horns provided by the pilot laboratory: the second Narda horn was used as well.

The series of measurements for each set-up consisted of three measurements in which one horn was used for transmission only, another one for receiving only and the last one both for transmitting and receiving. For the second group of horns (all those horn provided by the pilot laboratory) the measurements were done also by changing the role of the receiver and transmitting horns. This gives, in principle, a second completely independent set, but also allows a “virtual” set of measurements in which each horn is both once transmitting and once receiving. All these aspects were taken into account in arriving at the final results.

The measurements at each requested frequency point were done using small scans of 2 GHz around the required value in steps of 0.25 GHz. The variations observed were used as an indication for the uncertainty of the method used.

Although it is possible to obtain the same separation between each pair of antennas, in practice small differences will be present. Assuming the gain of each horn is independent of distance (justified at large distances), an exact formula can be derived for each horn based on a set of three relevant measurements. If G1 denotes the gain of the DUT, one gets the following result:

$$G1 = (4*pi*f/c)*(R12*R13/R23)*sqrt[(P12*P13)/(P23*Pref)]$$

where f = frequency of the signal
c = velocity of radiation

Rxy = distance between front faces of horn x (transmitting) and horn y (receiving)

Pxy = transmitted power between horn x (transmitting) and horn y (receiving)

Pref = transmitted power when waveguides are directly connected without horns.

The reflection coefficients of the horns used were determined using a Wiltron 360 VNA (up to 40 GHz) and a Flann Silver calibration kit. At a distance of about 0.5 m an absorbing pyramidal square (peak height 30 cm; 60 cm x 60 cm) was placed in front of the horn to absorb all emitted radiation.

In addition to the official measurements some investigations were done into the sensitivity for non-alignment. The receiver horn was displaced, in the plane perpendicular to the bore axes of the two horns, by 5 mm in the horizontal and in the vertical plane. The change in the transmission for the Scientific Atlanta horn was unexpectedly large (up to 0.6 dB), while the Narda horn showed a deviation of less than 0.1 dB.

There is a significant difference in measured gain depending on the exact combination of horns used, even in which they operate (transmit and/or receive). Hence, a much more extensive investigation should be carried out to obtain the main sources for this inconsistency.

The measurements were performed in May 1999 and the ambient conditions during the measurements were: temperature: (22 ± 2)ºC, relative air humidity: (45 ± 10)%

NIST

The on-axis gain of the antennas was measured using a generalized three-antenna measurement technique [2]. An extrapolation measurement technique was used to evaluate and correct for near-zone and multiple reflection effects in the measured data. The antennas were nominally linearly polarized. The gain and reflection coefficients were measured at the waveguide port of the antenna. Stepped frequency gain measurements were made from 26.5 to 40 GHz in 50 MHz steps and corrected using the fixed gain measurements. In addition to the two comparison antennas, the third antenna used was another Scientific Atlanta model 12A-26 horn belonging to NIST. Corrections for mismatch were also applied.

BNM-LCIE

The horn antennas have been measured in the fully anechoic chamber recently built at LCIE. Its dimensions are: 2.4 m height x 2.6 m width x 3.6 m depth. The measurement technique used is the standard site method involving three horn antennas. At each operating frequency, the attenuation parameter of the chamber as well as the reflection coefficient of the horn antenna have been considered in the calculation of the horn antenna gain. The measurement bench was made using a waveguide microwave generator, an amplifier, a directional coupler, different adapters and cables, a

spectrum analyser and two horn antennas. The measurement separation range used between horn antennas was 1.7 m at 26.5 GHz, 2.3 m at 33 GHz and 2.7 m at 40 GHz. The complex reflection coefficients of the horn antenna were measured using a heterodyne vector network analyser HP8510C.

No extrapolation or near-zone corrections were applied.

KRISS

The three antenna method based on the extrapolation technique was used to measure the gain of the antennas. The chamber is covered with 48" radiation absorbing material and the dimensions are 13 m long, 10 m wide, and 7.5 m high.

A synthesized signal generator (HP83640A), an amplifier (HP83050A), a directional coupler, and an isolator are used to supply the RF signal to the transmitting antenna and a microwave receiver (HP8530A) is connected to the receiving antenna through a frequency converter (HP8511B). The reflection coefficients of each antenna, the transmitter, and the receiver are measured using a network analyzer (HP8510C) calibrated using the TRL method.

The initial and final separations between the transmitting antenna and the receiving antennas are 51.6 cm and 251.6 cm for antenna pair 1 and 2, and 64.9 cm and 264.9 cm for antenna pair 3. The number of measurement positions is about 1900.

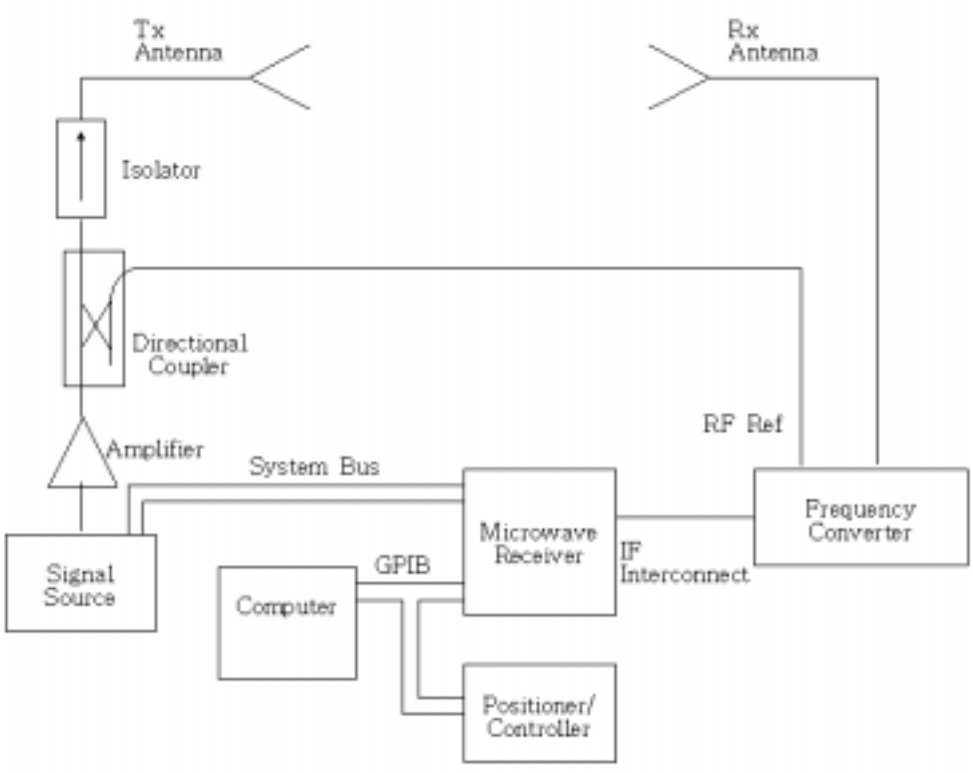

Fig. 1. Block diagram of the measurement set-up.

For the measurement set-up described above, the product of the gains of the antennas is given by

$$
\begin{aligned}
G_1 G_2 &= \left(\frac{4\pi}{\lambda}\right)^2 \frac{r^2 P_{R12}}{P_D} M_{12} \\
G_1 G_3 &= \left(\frac{4\pi}{\lambda}\right)^2 \frac{r^2 P_{R13}}{P_D} M_{13} \\
G_2 G_3 &= \left(\frac{4\pi}{\lambda}\right)^2 \frac{r^2 P_{R23}}{P_D} M_{23}
\end{aligned}
\qquad (1)
$$

where r is the distance between the apertures of the Tx and Rx antennas, P_D is the received power when the transmitting and receiving waveguides are connected directly, P_{Rij} is the received power when the two antennas are connected to the transmitting and receiving waveguides, respectively, and M_{ij} is the mismatch correction factor.

The gain of the AUT can be obtained by

$$
\begin{aligned}
G_1(dB) &= R_{12}(dB) + R_{13}(dB) - R_{23}(dB) + M_1(dB) \\
G_2(dB) &= R_{12}(dB) + R_{23}(dB) - R_{13}(dB) + M_2(dB) \\
G_3(dB) &= R_{13}(dB) + R_{23}(dB) - R_{12}(dB) + M_3(dB)
\end{aligned}
\qquad (2)
$$

$$
\begin{aligned}
M_1 &= \sqrt{\frac{M_{12} M_{13}}{M_{23}}} = \frac{|1-\Gamma_G\Gamma_1|^2 |1-\Gamma_2\Gamma_L|}{(1-|\Gamma_1|^2)|1-\Gamma_G\Gamma_2||1-\Gamma_G\Gamma_L|} \\
M_2 &= \sqrt{\frac{M_{12} M_{23}}{M_{13}}} = \frac{|1-\Gamma_G\Gamma_2||1-\Gamma_2\Gamma_L|}{(1-|\Gamma_2|^2)|1-\Gamma_G\Gamma_L|} \\
M_3 &= \sqrt{\frac{M_{13} M_{23}}{M_{12}}} = \frac{|1-\Gamma_3\Gamma_L|^2||1-\Gamma_G\Gamma_2|}{(1-|\Gamma_3|^2)|1-\Gamma_G\Gamma_L||1-\Gamma_2\Gamma_L|}
\end{aligned}
$$

where

$R_{ij} = \lim_{r\to\infty} 4\pi/\lambda \cdot \sqrt{r^2 P_{Rij}/P_D}$,

M_i mismatch correction factor,
Γ_1 reflection coefficient of the AUT 1 (Scientific Atlanta 12A-26, marked “INT”),
Γ_2 reflection coefficient of the AUT 2 (Narda V637 , marked “INT”),
Γ_3 reflection coefficient of the AUT 3 (Narda V637 , marked “C”),
Γ_G reflection coefficient of the transmitter,
Γ_L reflection coefficient of the receiver.

Summary of Corrections Applied

Laboratory	Near-Zone Correction	Mismatch Correction
NPL	Yes – Extrapolation method used	Corrected for mismatch
NMi-VSL	No – Measured at 4.2 m	No correction made
NIST	Yes – Extrapolation method used	Corrected for mismatch
BNM-LCIE	No – Measured at 1.7 m at 26.5 GHz, 2.3 m at 33 GHz and 2.7 m at 40 GHz	Corrected for mismatch
KRISS	Yes – Extrapolation method used	Corrected for mismatch

7. MEASUREMENT RESULTS

The results presented by the participating laboratories are given in the tables below. The weighted mean is given in the tables for the gain, having first excluded outliers, which are indicated by italic text. The unweighted mean is given for the real and imaginary parts of the reflection coefficient. Equations for the calculation of the mean values and the rationale a weighted mean for the gain and an unweighted one for the reflection coefficient are given in the next section.

The uncertainty originally reported by BNM-LCIE (0.36 dB at all frequencies) and NIST (0.08 dB for 3σ) were updated after the Draft A report was circulated, as the uncertainty calculation had not been made in accordance with the requirements of the Guide to the Expression of Uncertainty in Measurement.

Table 1: Gain results for SA horn 12A-26 s/n 16056HC.
Values in italics were excluded from the calculation of the mean, which is weighted.

Laboratory	26.5 GHz Gain [dB]	Uncert. 1 σ [dB]	33.0 GHz Gain [dB]	Uncert. 1 σ [dB]	40.0 GHz Gain [dB]	Uncert. 1 σ [dB]
NPL (1)	23.385	0.025	24.428	0.025	25.055	0.025
NMi-VSL	23.40	0.25	24.31	0.25	25.14	0.25
NIST	23.48	0.031	24.55	0.031	25.13	0.031
BNM-LCIE	23.36	0.145	24.12	0.081	*24.42*	0.325
NPL (2)	23.378	0.025	24.457	0.025	25.033	0.025
KRISS	23.490	0.125	24.510	0.207	25.086	0.394
Mean	23.421		24.464		25.078	

Table 2: Gain results for Narda horn V637 marked "INT".
Values in italics were excluded from the calculation of the mean, which is weighted.

Laboratory	26.5 GHz Gain [dB]	Uncert. 1 σ [dB]	33.0 GHz Gain [dB]	Uncert. 1 σ [dB]	40.0 GHz Gain [dB]	Uncert. 1 σ [dB]
NPL (1)	14.848	0.025	16.520	0.025	18.080	0.025
NMi-VSL	*14.70*	0.25	16.56	0.25	18.28	0.25
NIST	14.87	0.031	16.64	0.031	18.22	0.031
BNM-LCIE	*14.50*	0.145	*16.11*	0.081	*16.70*	0.325
NPL (2)	14.858	0.025	16.515	0.025	18.074	0.025
KRISS	14.881	0.126	16.626	0.207	18.151	0.394
Mean	14.860		16.566		18.134	

Table 3: Real part of the reflection coefficient for SA horn 12A-26 s/n 16056HC.
Values in italics were excluded from the calculation of the mean.

Laboratory	26.5 GHz Real Part	Uncert. 1 σ	33.0 GHz Real Part	Uncert. 1 σ	40.0 GHz Real Part	Uncert. 1 σ
NPL (1)	0.054	0.004	0.036	0.004	0.033	0.004
NMi-VSL	0.052	0.01	0.035	0.01	0.035	0.01
NIST	0.047	0.015	*0.025*	0.015	0.036	0.015
BNM-LCIE	0.04637	0.0020	0.03947	0.0019	0.03779	0.0040
NPL (2)	0.053	0.004	0.036	0.004	*0.029*	0.004
KRISS	0.0529	0.005	0.0343	0.004	0.0353	0.004
Mean	0.050		0.036		0.035	

Table 4: Imaginary part of the reflection coefficient for SA horn 12A-26 s/n 16056HC.
Values in italics were excluded from the calculation of the mean.

Laboratory	26.5 GHz Imag. Part	Uncert. 1 σ	33.0 GHz Imag. Part	Uncert. 1 σ	40.0 GHz Imag. Part	Uncert. 1 σ
NPL (1)	0.040	0.004	0.020	0.004	0.007	0.004
NMi-VSL	0.040	0.01	0.022	0.01	0.009	0.01
NIST	0.042	0.01	0.022	0.01	*0.020*	0.01
BNM-LCIE	*0.03461*	0.0040	*0.03043*	0.0040	-0.00052	0.0019
NPL (2)	0.041	0.004	0.021	0.004	0.009	0.004
KRISS	0.0388	0.006	0.0189	0.005	0.0050	0.005
Mean	0.040		0.021		0.005	

Table 5: Real part of the reflection coefficient for Narda horn V637 marked "INT".
Values in italics were excluded from the calculation of the mean.

Laboratory	26.5 GHz Real Part	Uncert. 1 σ	33.0 GHz Real Part	Uncert. 1 σ	40.0 GHz Real Part	Uncert. 1 σ
NPL (1)	-0.024	0.004	0.026	0.004	-0.007	0.004
NMi-VSL	-0.025	0.01	0.025	0.01	-0.007	0.01
NIST	*-0.030*	0.015	*0.019*	0.015	*0.009*	0.015
BNM-LCIE	*-0.02085*	0.0040	0.02558	0.0040	-0.00453	0.0011
NPL (2)	-0.024	0.004	0.028	0.004	-0.009	0.004
KRISS	-0.0247	0.005	0.0259	0.004	-0.0036	0.004
Mean	-0.025		0.026		-0.006	

Table 6: Imaginary part of the reflection coefficient for Narda horn V637 marked "INT.
Values in italics were excluded from the calculation of the mean.

Laboratory	26.5 GHz Imag. Part	Uncert. 1 σ	33.0 GHz Imag. Part	Uncert. 1 σ	40.0 GHz Imag. Part	Uncert. 1 σ
NPL (1)	0.031	0.004	0.001	0.004	-0.015	0.004
NMi-VSL	0.030	0.01	0.001	0.01	-0.014	0.01
NIST	0.030	0.01	0.002	0.01	*-0.005*	0.01
BNM-LCIE	0.02691	0.0019	-0.00058	0.0019	-0.01819	0.0043
NPL (2)	0.031	0.004	0.002	0.004	-0.013	0.004
KRISS	0.0291	0.004	0.0025	0.005	-0.0152	0.004
Mean	0.029		0.001		-0.015	

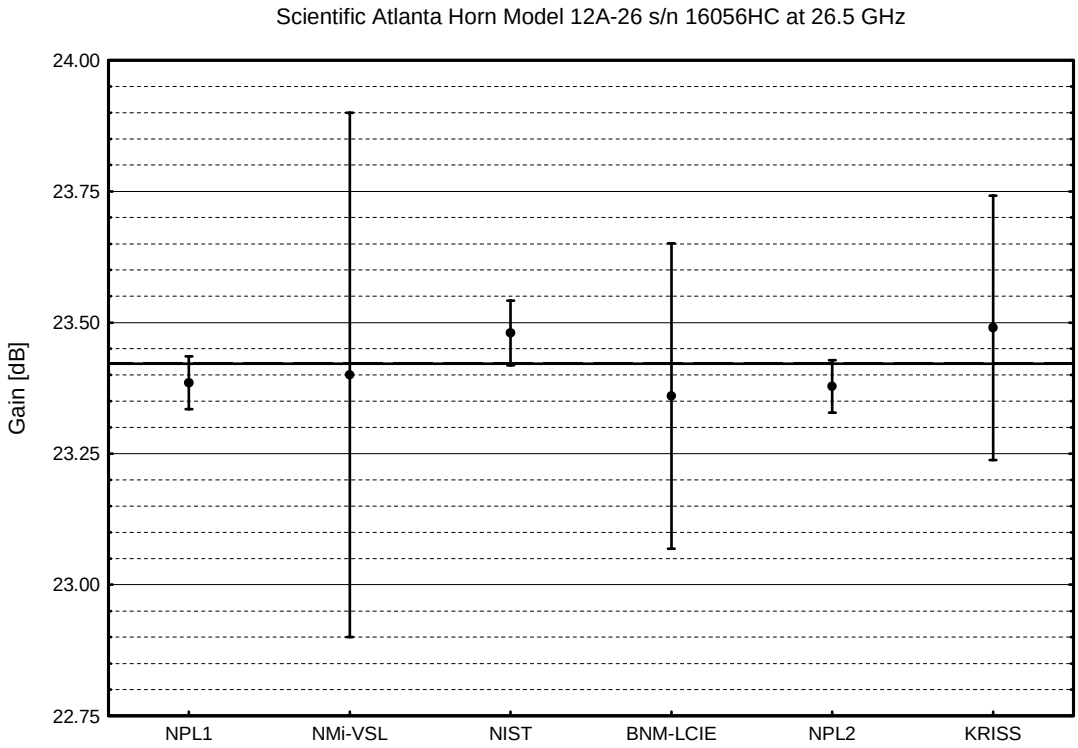

Figure 2a: The gain of the Scientific Atlanta horn at 26.5 GHz.

The weighted mean is shown as a solid line and the unweighted mean as a dashed line, which is virtually coincident with it. The uncertainty is for k=2.

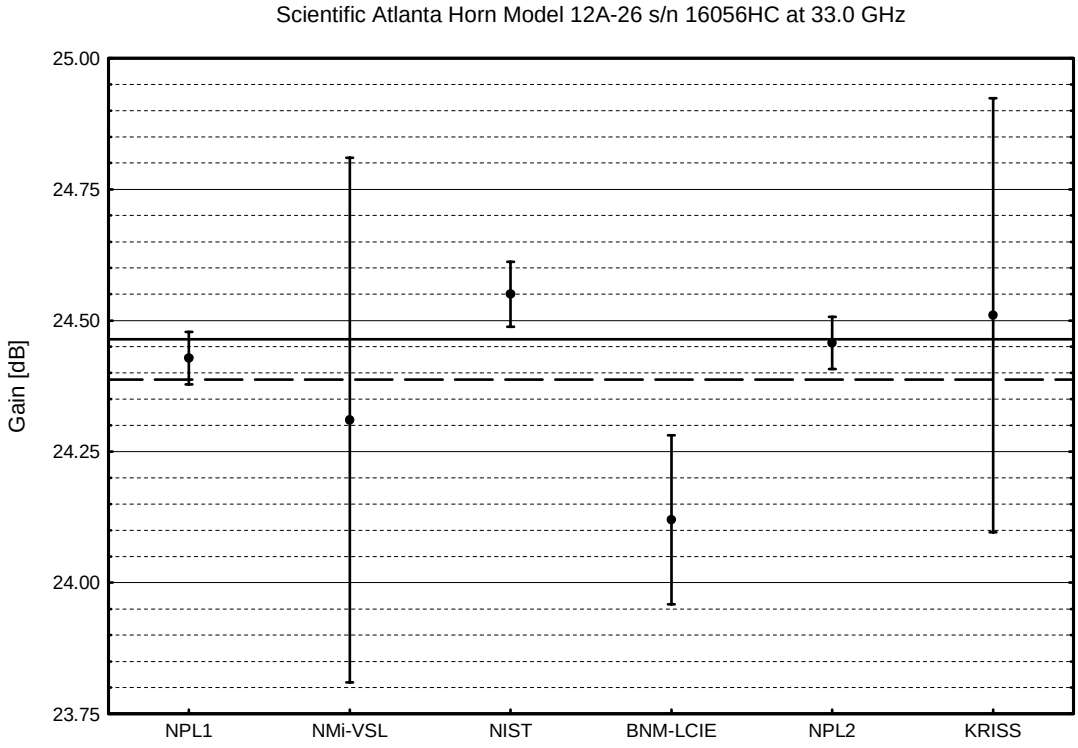

Figure 2b: The gain of the Scientific Atlanta horn at 33.0 GHz.

The weighted mean is shown as a solid line and the unweighted mean as a dashed line. The uncertainty is for k=2.

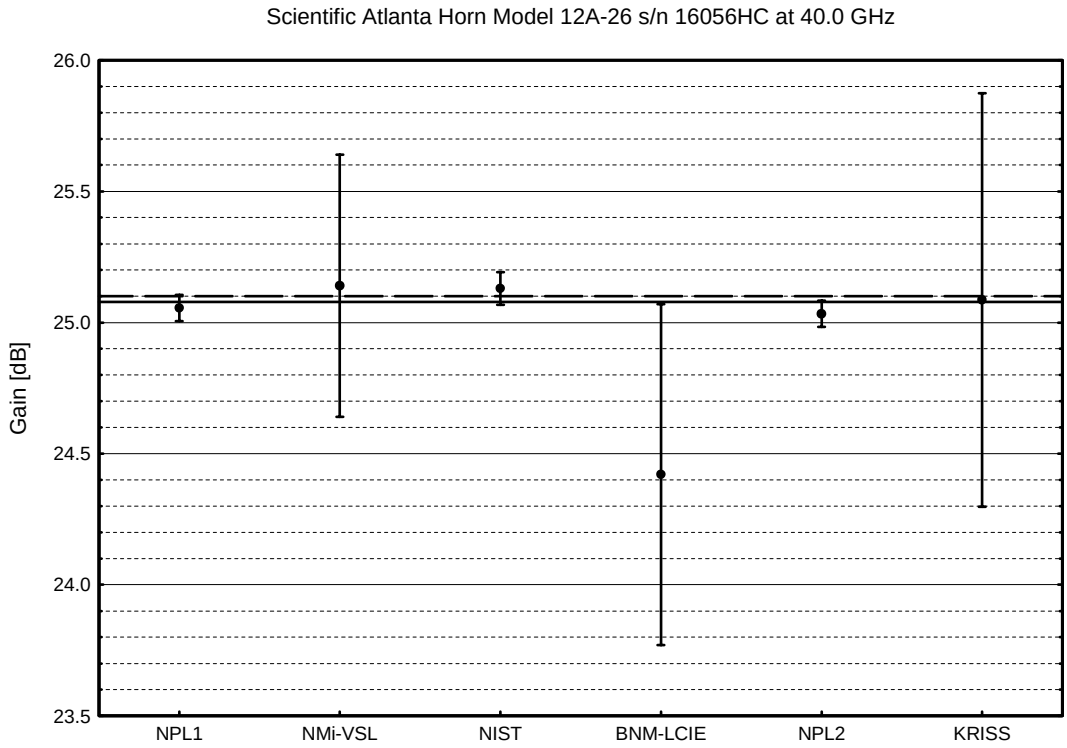

Figure 2c: The gain of the Scientific Atlanta horn at 40.0 GHz.

The weighted mean is shown as a solid line and the unweighted mean as a dashed line. Both exclude the BNM-LCIE value. The uncertainty is for k=2.

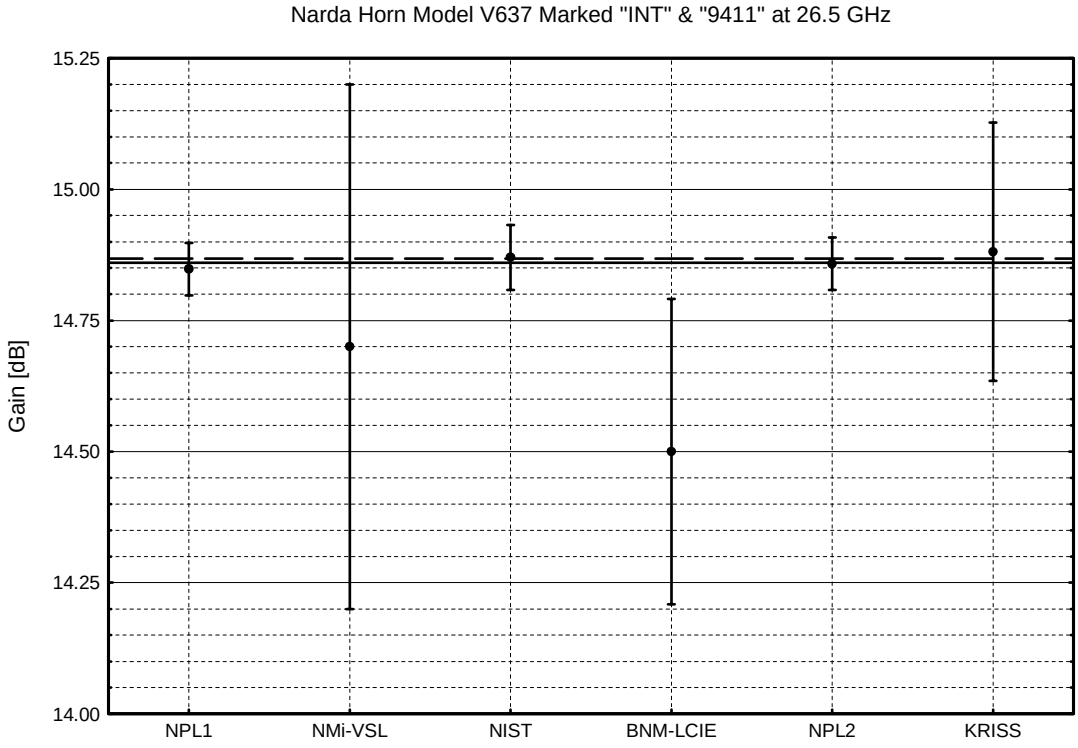

Figure 3a: The gain of the Narda horn at 26.5 GHz.

The weighted mean is shown as a solid line and the unweighted mean as a dashed line. Both means exclude the NMi-VSL and BNM-LCIE values. The uncertainty is for k=2.

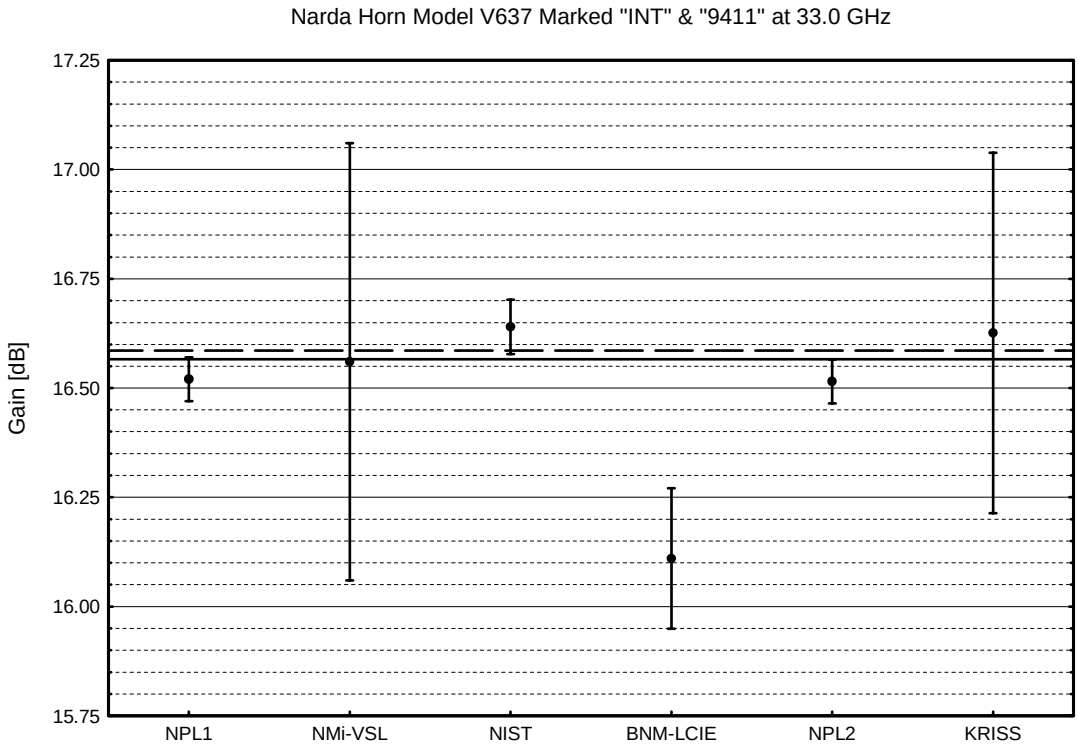

Figure 3b: The gain of the Narda horn at 33.0 GHz.

The weighted mean is shown as a solid line and the unweighted mean as a dashed line. Both exclude the BNM-LCIE value. The uncertainty is for k=2.

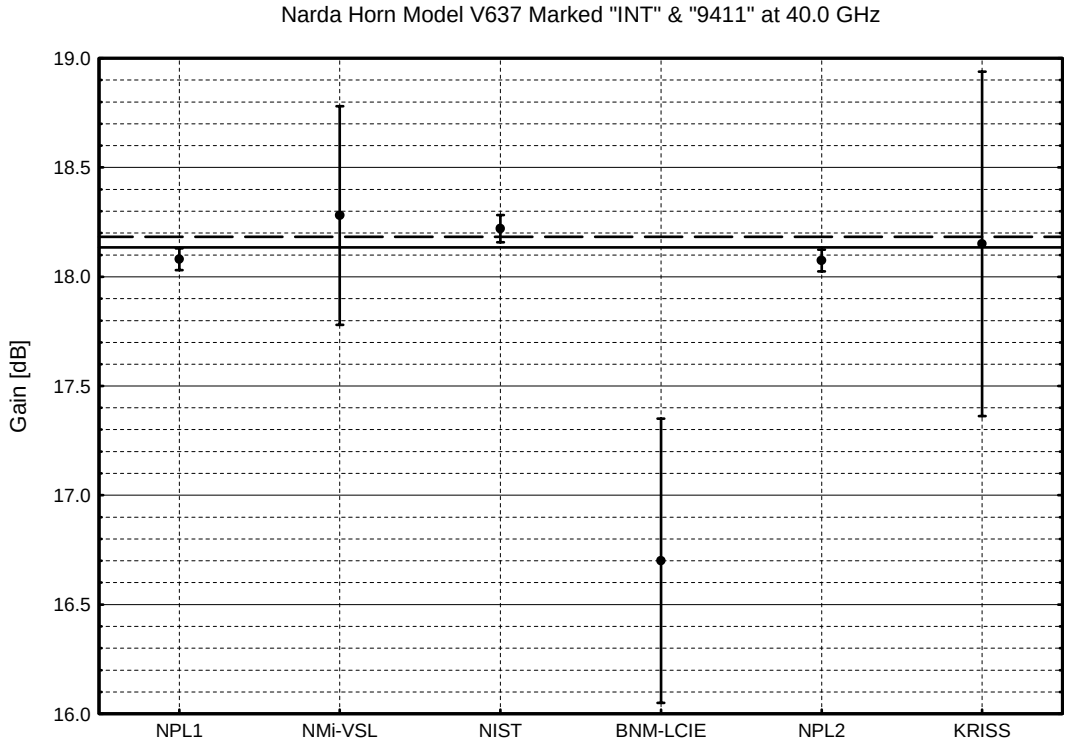

Figure 3c: The gain of the Narda horn at 40.0 GHz.

The weighted mean is shown as a solid line and the unweighted mean as a dashed line. Both exclude the BNM-LCIE value. The uncertainty is for k=2.

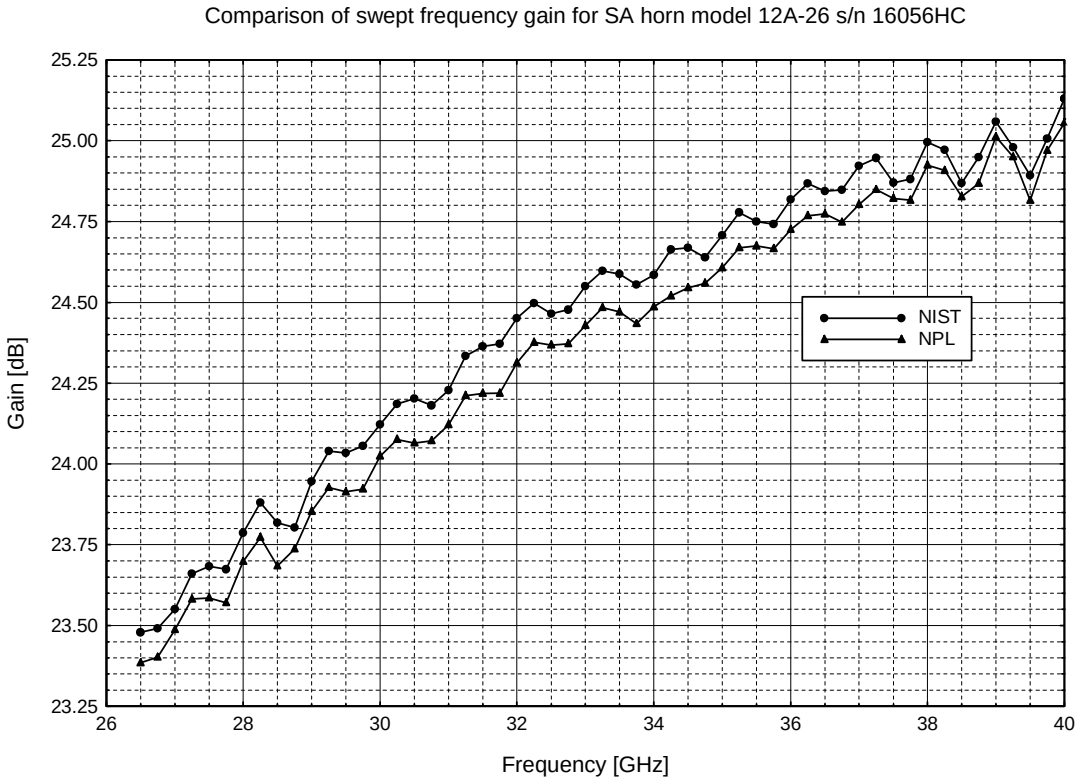

Figure 4a: The swept frequency gain of the SA horn as measured by NPL and NIST.

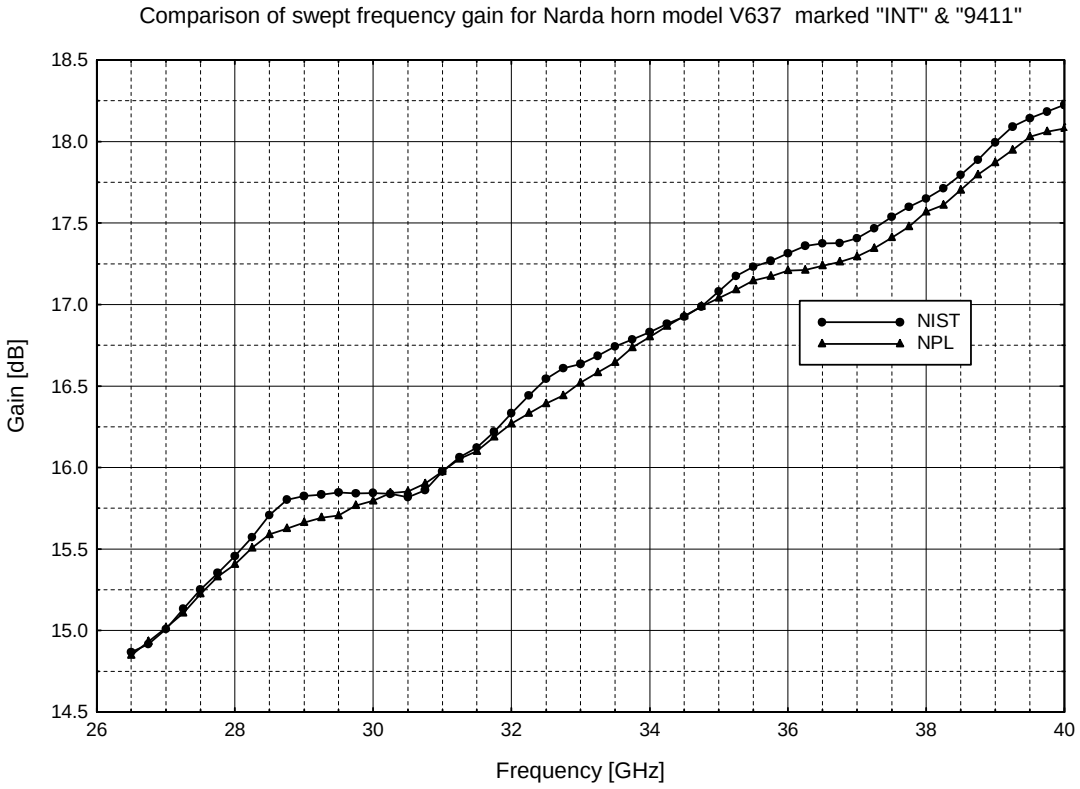

Figure 4b: The swept frequency gain of the Narda horn as measured by NPL and NIST.

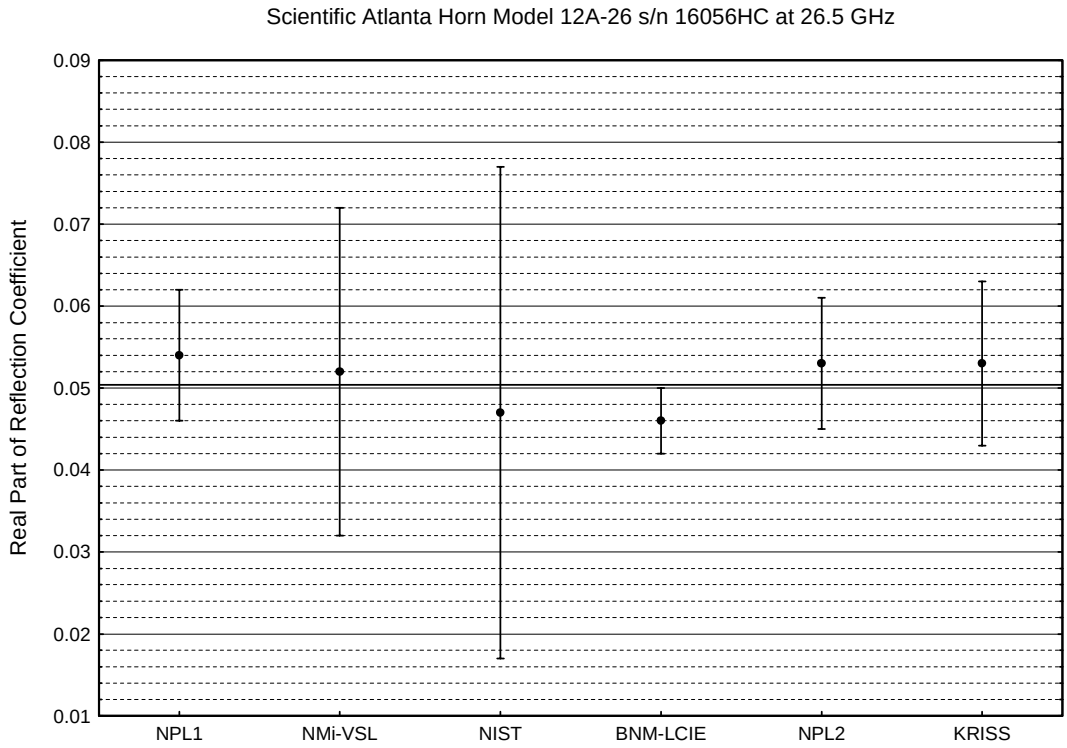

Figure 5a: The real part of the reflection coefficient of the SA horn at 26.5 GHz.
The unweighted mean is shown as a solid line. The uncertainty is for k=2.

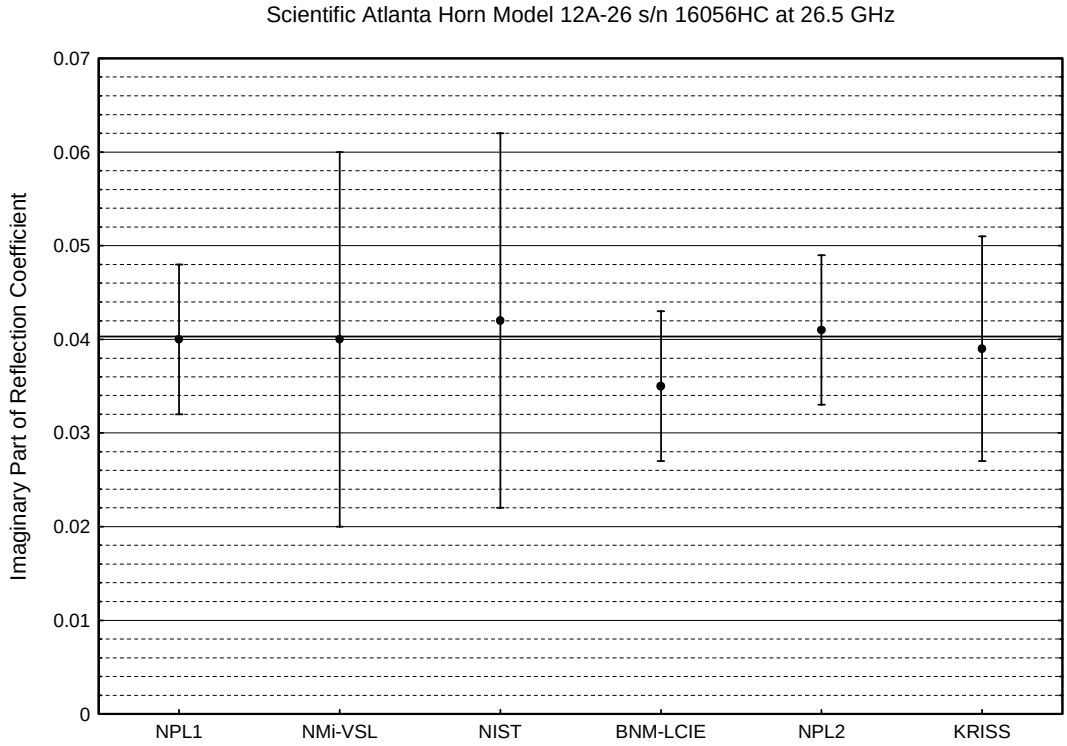

Figure 5b: The imaginary part of the reflection coefficient of the SA horn at 26.5 GHz.
The unweighted mean excluding the BNM-LCIE value is shown as a solid line. The uncertainty is for k=2.

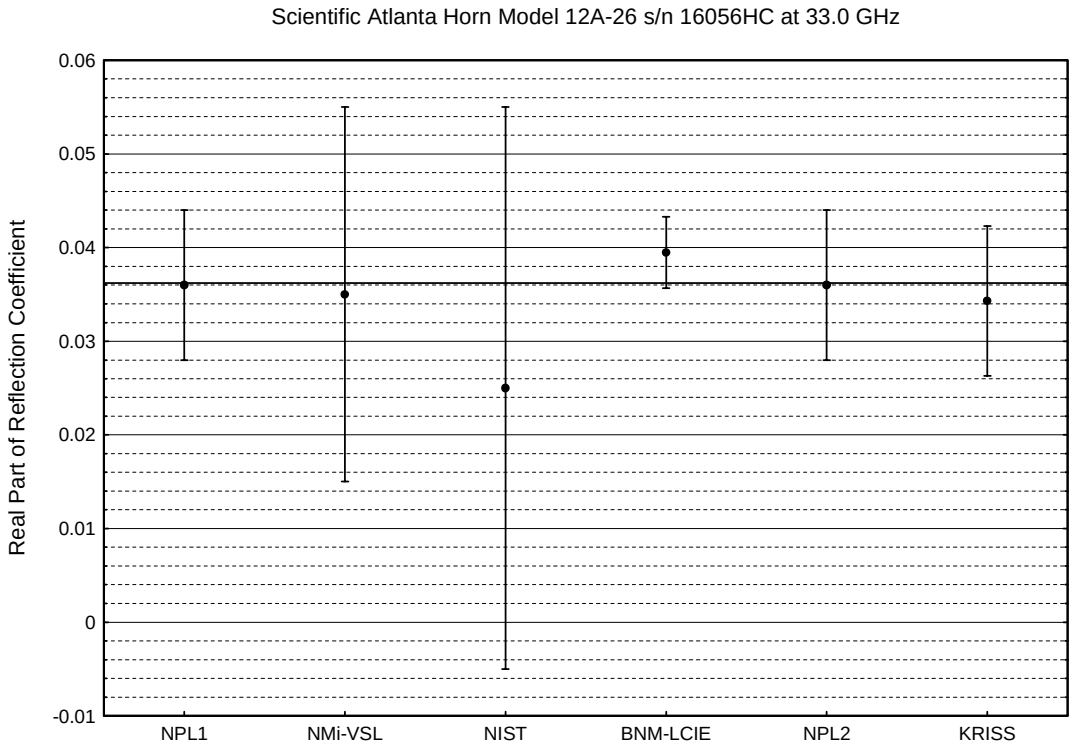

Figure 6a: The real part of the reflection coefficient of the SA horn at 33.0 GHz.

The unweighted mean excluding the NIST value is shown as a solid line. The uncertainty is for k=2.

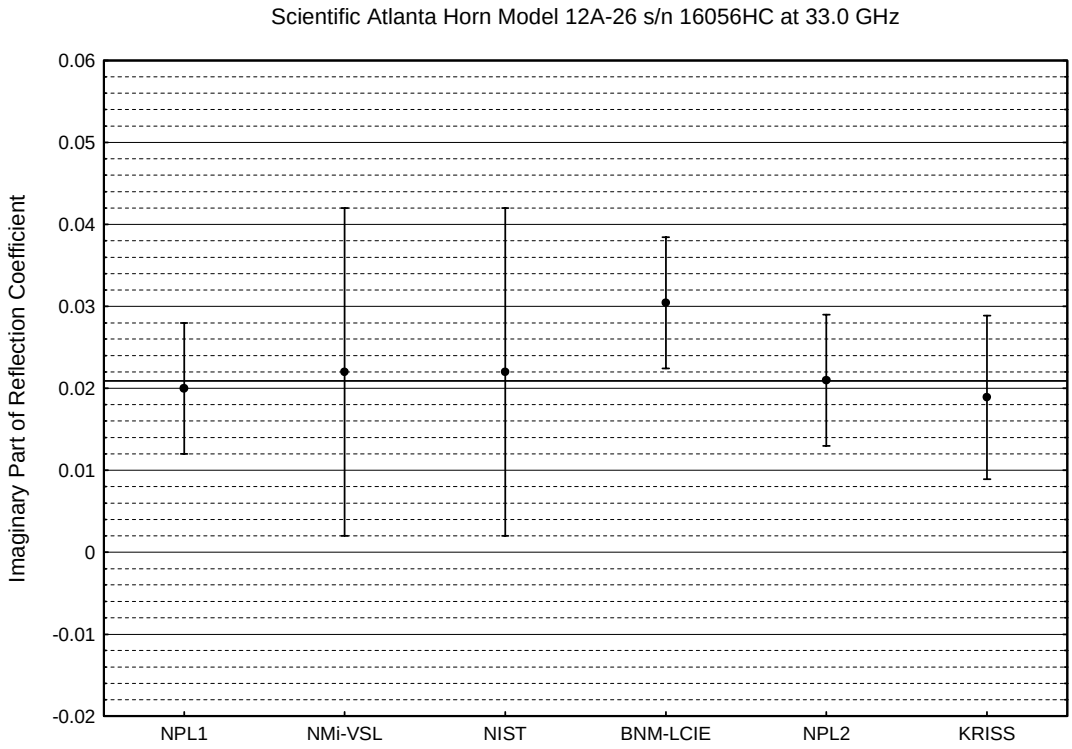

Figure 6b: The imaginary part of the reflection coefficient of the SA horn at 33.0 GHz.

The unweighted mean excluding the BNM-LCIE value is shown as a solid line. The uncertainty is for k=2.

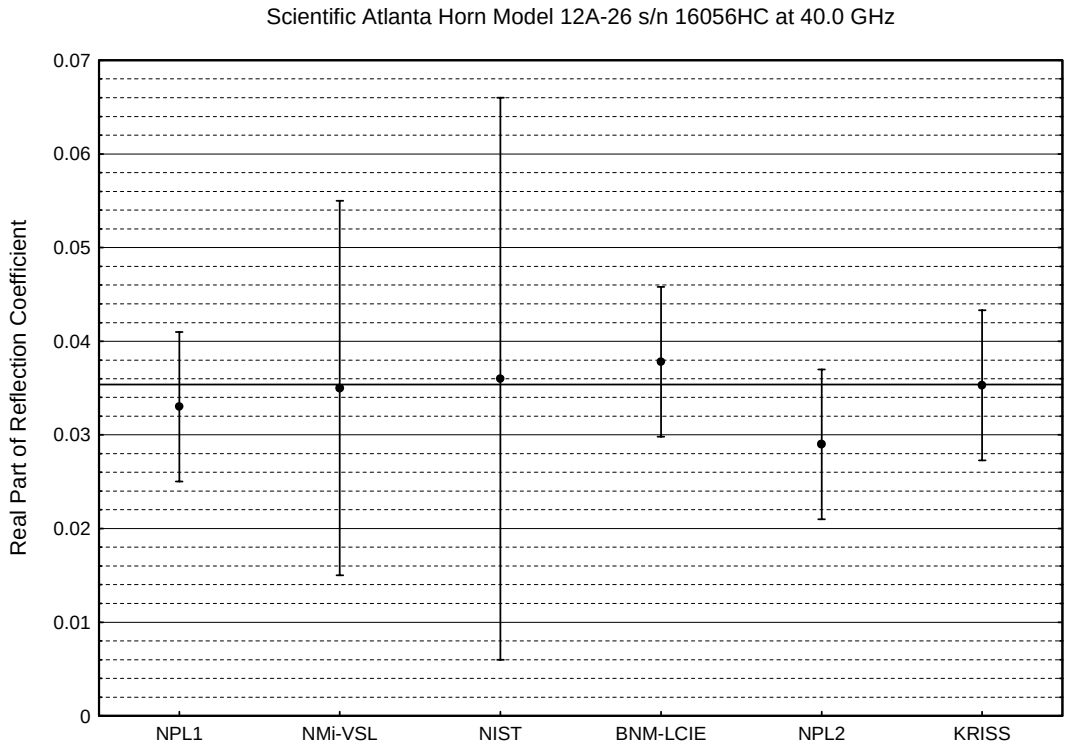

Figure 7a: The real part of the reflection coefficient of the SA horn at 40.0 GHz.

The unweighted mean excluding the NPL 2 value is shown as a solid line. The uncertainty is for k=2.

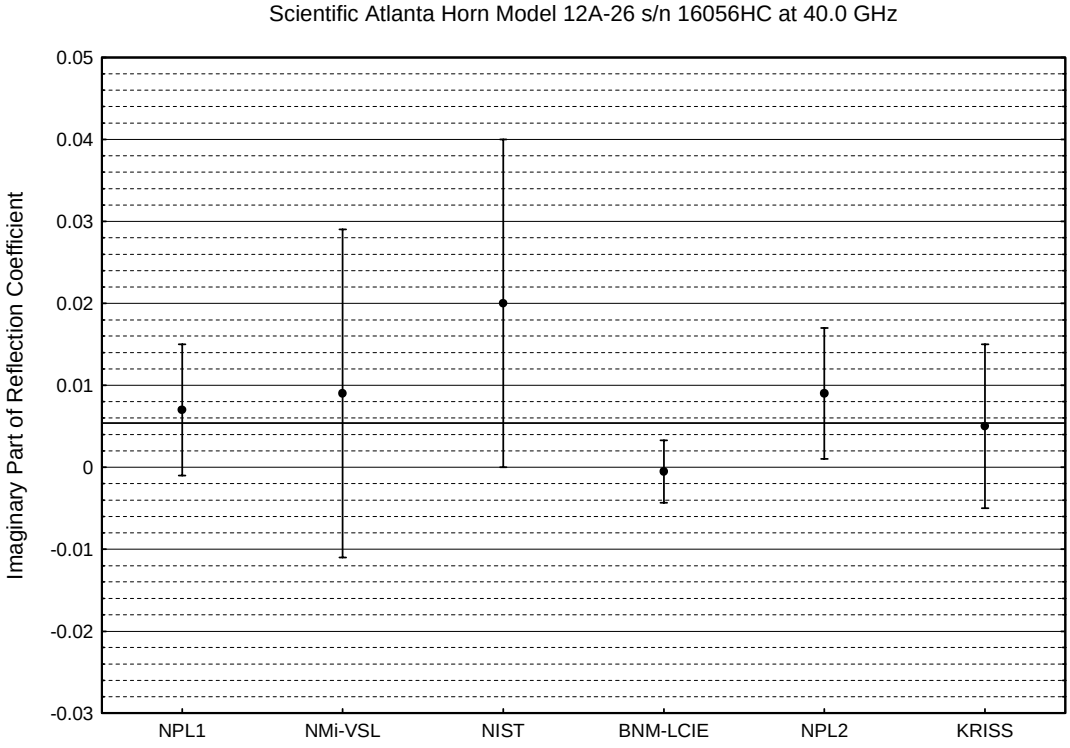

Figure 7b: The imaginary part of the reflection coefficient of the SA horn at 40.0 GHz.

The unweighted mean excluding the NIST value is shown as a solid line. The uncertainty is for k=2.

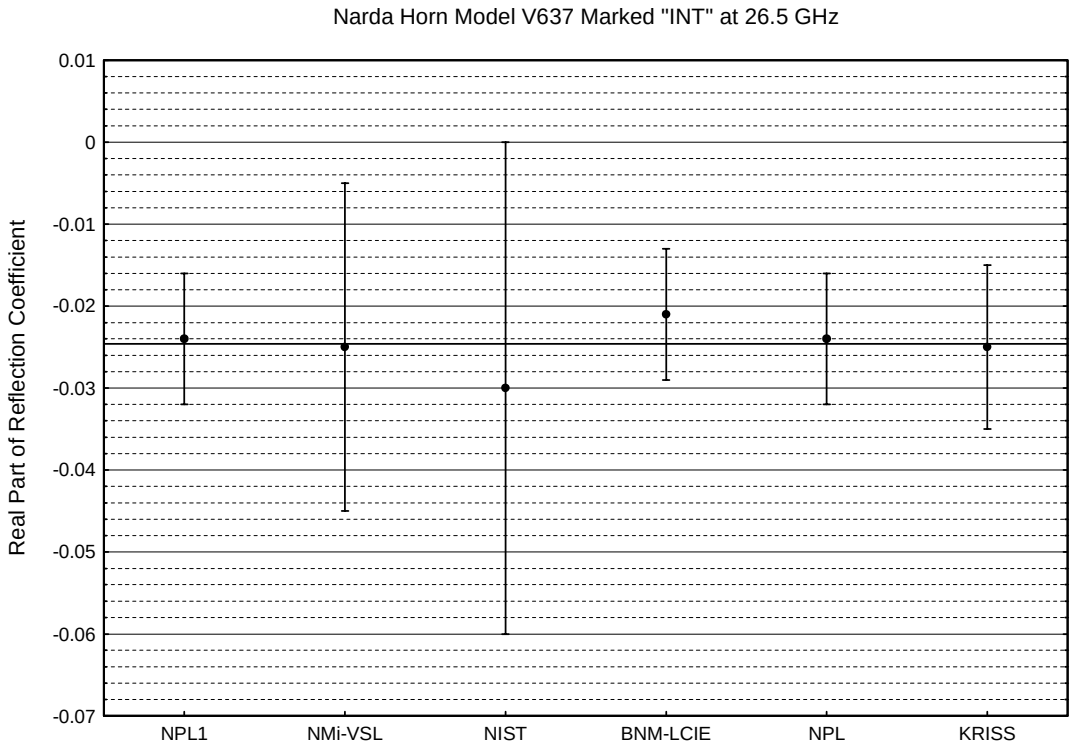

Figure 8a: The real part of the reflection coefficient of the Narda horn at 26.5 GHz.

The unweighted mean excluding the NIST and BNM-LCIE values is shown as a solid line. The uncertainty is for k=2.

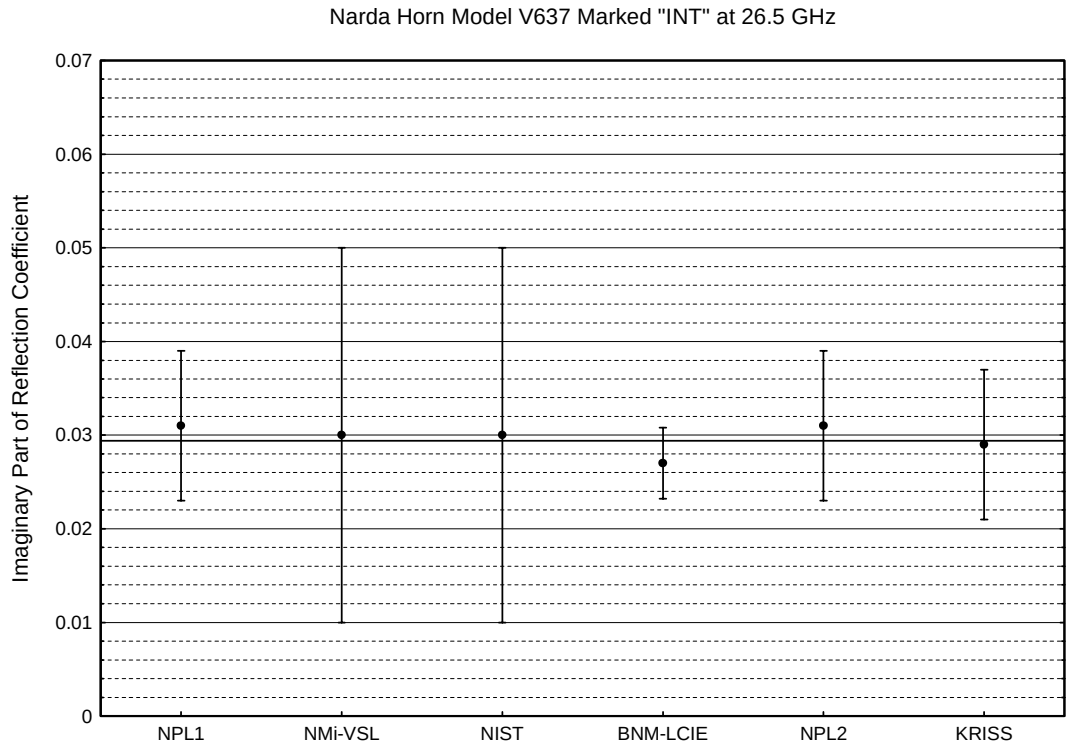

Figure 8b: The imaginary part of the reflection coefficient of the Narda horn at 26.5 GHz.

The unweighted mean is shown as a solid line. The uncertainty is for k=2.

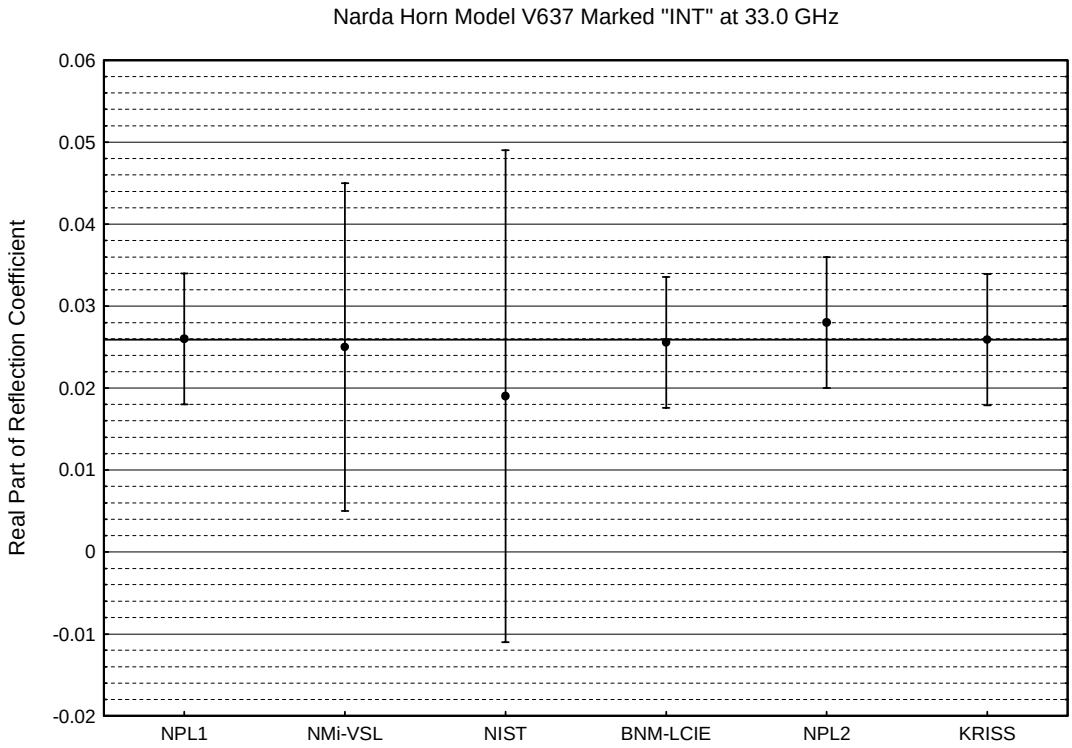

Figure 9a: The real part of the reflection coefficient of the Narda horn at 33.0 GHz.

The unweighted mean excluding the NIST value is shown as a solid line. The uncertainty is for k=2.

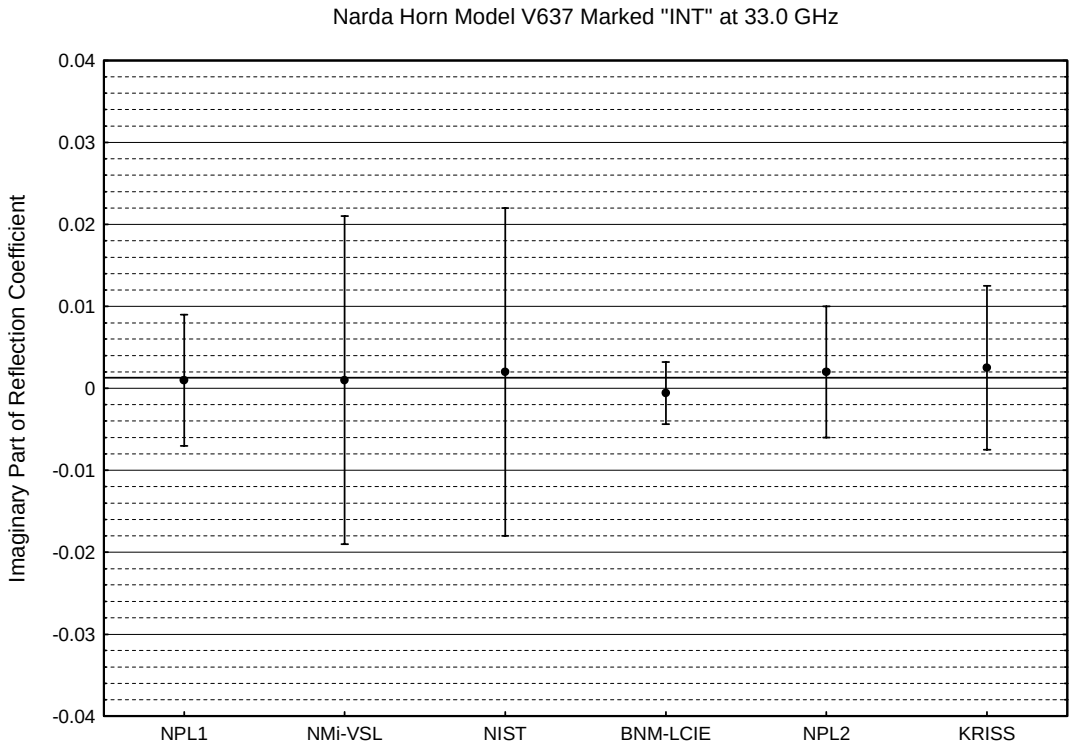

Figure 9b: The imaginary part of the reflection coefficient of the Narda horn at 33.0 GHz.

The unweighted mean is shown as a solid line. The uncertainty is for k=2.

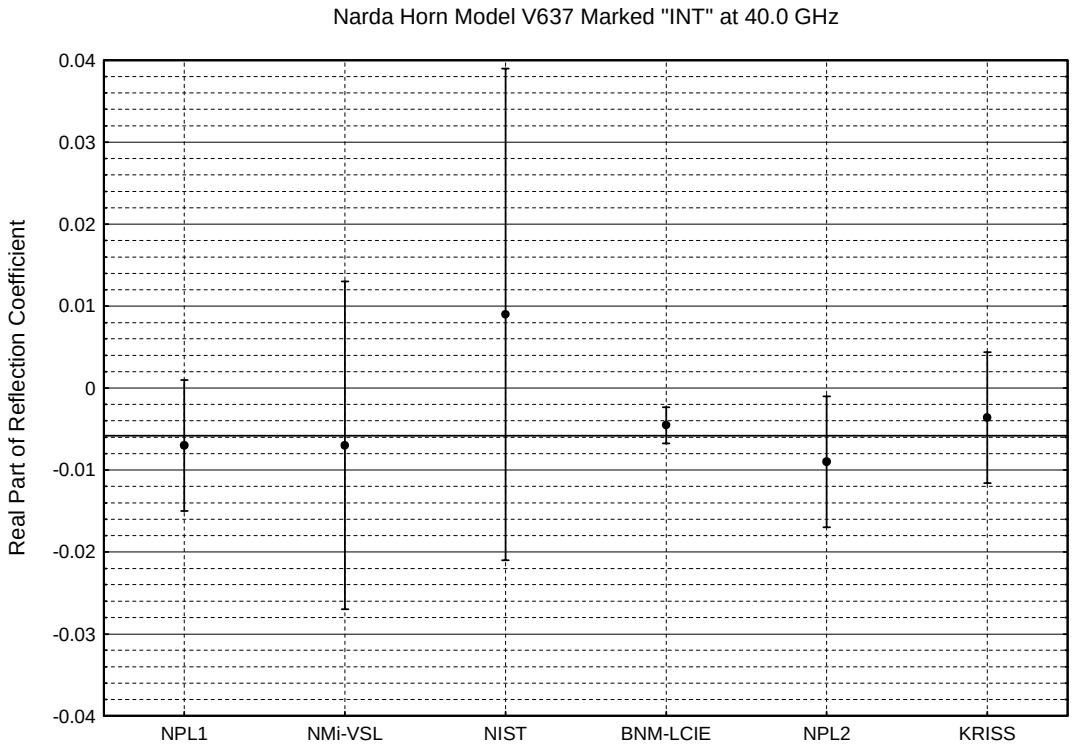

Figure 10a: The real part of the reflection coefficient of the Narda horn at 40.0 GHz.

The unweighted mean excluding the NIST value is shown as a solid line. The uncertainty is for k=2.

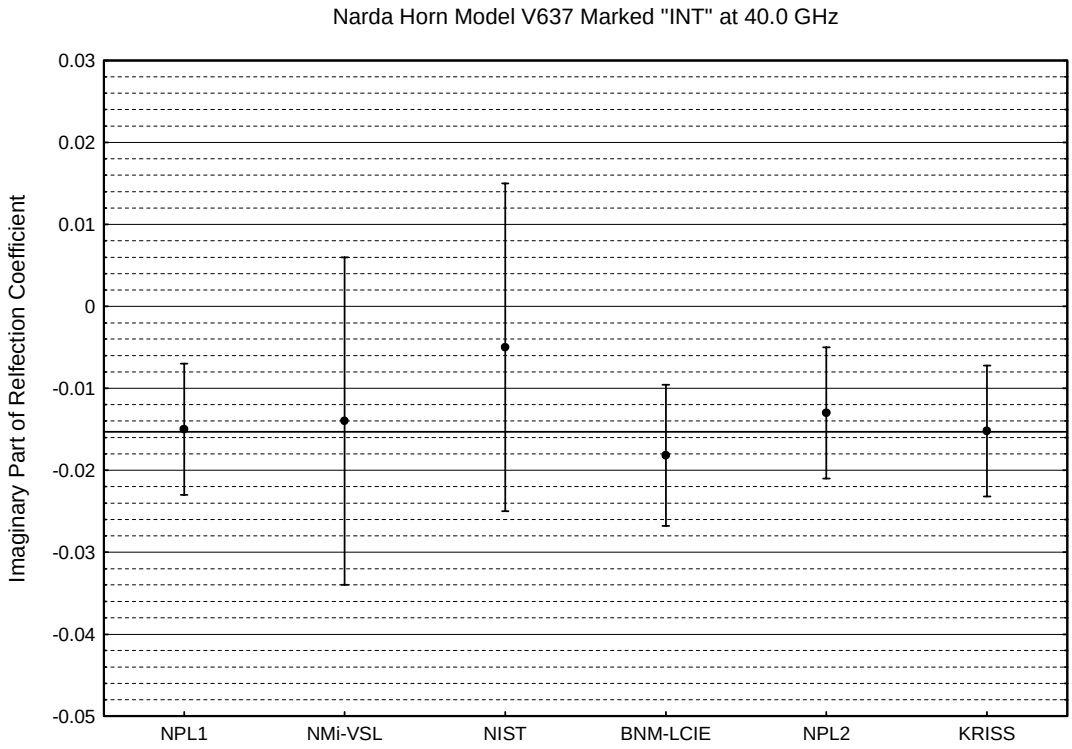

Figure 10b: The imaginary part of the reflection coefficient of the Narda horn at 40.0 GHz.

The unweighted mean excluding the NIST value is shown as a solid line. The uncertainty is for k=2.

8. MEAN VALUES AND KEY COMPARISON REFERENCE VALUES

The mean values given in the tables and graphs above have been calculated using the method proposed by J Randa of NIST [3] for determining outliers and calculating Key Comparison Reference Values.

For each parameter, the Median of Absolute Deviations (MAD) have been determined and used to test each participant's reported value to see if it is an outlier, according to the method described in [3]. The mean values have been calculated, having excluded the outliers identified in the previous step, and those outliers are identified in the tables by the entry being in italics. A note has also been included beneath each graph to indicate which values have been excluded in the evaluation of the mean.

The most contentious issue is whether to use a weighted mean or an unweighted one, as discussed in [3]. In this report, the weighted mean has been calculated for the gain values and the unweighted mean for the real and imaginary parts of the reflection coefficients. The rationale for this choice is that the reported uncertainties for the gain values vary greatly between participants and also not all participants performed a near-zone correction, either by extrapolation or calculation. This means that some of the reported values have a significant systematic uncertainty component that would unduly influence the mean if account were not taken of the associated uncertainty. The Key Comparison Reference Value (KCRV) for an unweighted mean has also been calculated and is given in the tables below for completeness.

For the real and imaginary parts of the reflection coefficient, the uncertainties quoted are all broadly similar, so an unweighted mean is more appropriate, though in fact it make little difference whether the weighted or unweighted mean is taken. The prime objective of the comparison was to measure the gain of the standard antennas and therefore degrees of equivalence have only been calculated for the gain.

For all evaluations of the median and S(MAD) during the identification of outliers, the two NPL values were averaged and the result treated as a single measurement:

$$\overline{NPL} = \frac{NPL(1) + NPL(2)}{2} \tag{3}$$

Once the median and S(MAD) had been calculated, the outlier test was applied to each of the NPL measurements separately, along with those from the other participants. Where one of the NPL values was identified as an outlier, it was excluded from the subsequent calculation of the mean value, but the other value was included provided it was not also an outlier.

The weighted KCRV is given by the following expression:

$$\overline{x_w} = \sum_{i=1}^{N} \frac{x_i}{u^2(x_i)} \times u^2(\overline{x_w}) \tag{4}$$

where x_i is the value reported by laboratory i and $u^2(x_i)$ is the square of the standard uncertainty reported by laboratory i. The uncertainty in the weighted KCRV is given by:

$$u^2(\overline{x_w}) = \frac{1}{\sum_{i=1}^{N} \left(\frac{1}{u^2(x_i)} \right)} \tag{5}$$

The unweighted KCRV is given by:

$$\overline{x_u} = \frac{1}{N} \sum_{i=1}^{N} x_i \tag{6}$$

and its uncertainty is:

$$u^2(\overline{x_u}) = \frac{1}{N^2} \sum_{i=1}^{N} u^2(x_i) \tag{7}$$

Note that the above equation for the uncertainty in the KCRV using an unweighted mean differs from that given by Randa in [3], but is consistent with equation 12 of [4]. Randa [3] gives the estimated standard deviation of the mean of the reported values as the uncertainty of the unweighted KCRV.

The degree of equivalence of each laboratory i with respect to the reference value is given by:

$$d_i = (x_i - \overline{x_w}) \tag{8}$$

The uncertainty in the degree of equivalence depends on whether x_i is an outlier or not. If x_i is an outlier, then the expanded uncertainty is given by:

$$u(d_i) = 2\sqrt{u^2(x_i) + u^2(\overline{x_w})} \tag{9}$$

for the weighted case and

$$u(d_i) = 2\sqrt{u^2(x_i) + u^2(\overline{x_u})} \tag{10}$$

for the unweighted case. If x_i is not an outlier, then the expanded uncertainty (k=2) for the unweighted case is given by:

$$u(d_i) = 2\sqrt{u^2(\overline{x_u}) + (1 - \frac{2}{N'}) \times u^2(x_i)} \tag{11}$$

where N' is the number of values excluding outliers. The expanded uncertainty (k=2) for the weighted case is:

$$u(d_i) = 2\sqrt{u^2(x_i) - u^2(\overline{x_w})} \tag{12}$$

The degree of equivalence between laboratory i and another laboratory j is given by:

$$d_{ij} = (x_i - x_j) \tag{13}$$

The expanded uncertainty (k=2) in the degree of equivalence between laboratories is given by:

$$u(d_{ij}) = 2\sqrt{u^2(x_i) + u^2(x_j)} \tag{14}$$

The equations above assume there is no correlation between the results reported by different laboratories.

The tables and graphs below give the KCRV (both weighted and unweighted mean) and degrees of equivalence for the gain of the two reference antennas.

KCRV (weighted mean) and Degree of Equivalence for Gain

			NPL(mean)		NMi-VSL		NIST		BNM-LCIE		KRISS	
Freq [GHz]	$\overline{x_w}$	$u(\overline{x_w})$	d_i	$u(d_i)$	d_i	$u(d_i)$	d_i	$u(d_i)$	d_i	$u(d_i)$	d_i	$u(d_i)$
26.5	14.860	0.038	-0.007	0.032	-0.160	0.501	0.010	0.049	-0.360	0.293	0.021	0.243
33.0	16.566	0.039	-0.049	0.032	-0.006	0.499	0.074	0.048	-0.456	0.166	0.060	0.410
40.0	18.134	0.039	-0.057	0.032	0.146	0.498	0.086	0.048	-1.434	0.651	0.017	0.787

Table 7: KCRV (weighted mean) and degree of equivalence for the Narda horn.
The uncertainty is for k=2.

			NPL(mean)		NMi-VSL		NIST		BNM-LCIE		KRISS	
Freq [GHz]	$\overline{x_w}$	$u(\overline{x_w})$	d_i	$u(d_i)$	d_i	$u(d_i)$	d_i	$u(d_i)$	d_i	$u(d_i)$	d_i	$u(d_i)$
26.5	23.421	0.038	-0.039	0.032	-0.021	0.499	0.059	0.049	-0.061	0.288	0.069	0.249
33.0	24.464	0.038	-0.022	0.033	-0.154	0.499	0.086	0.049	-0.344	0.157	0.046	0.412
40.0	25.078	0.039	-0.034	0.032	0.062	0.498	0.052	0.048	-0.658	0.651	0.008	0.787

Table 8: KCRV (weighted mean) and degree of equivalence for the SA horn.
The uncertainty is for k=2.

KCRV (unweighted mean) and Degree of Equivalence for Gain

			NPL(mean)		NMi-VSL		NIST		BNM-LCIE		KRISS	
Freq [GHz]	$\overline{x_u}$	$u(\overline{x_u})$	d_i	$u(d_i)$	d_i	$u(d_i)$	d_i	$u(d_i)$	d_i	$u(d_i)$	d_i	$u(d_i)$
26.5	14.868	0.086	0.015	0.091	0.168	0.507	0.002	0.093	0.368	0.303	0.013	0.166
33.0	16.586	0.163	0.068	0.167	0.026	0.389	0.054	0.169	0.476	0.229	0.040	0.334
40.0	18.182	0.234	0.105	0.237	0.098	0.424	0.038	0.238	1.482	0.691	0.031	0.604

Table 9: KCRV (unweighted mean) and degree of equivalence for the Narda horn.
The uncertainty is for k=2.

			NPL(mean)		NMi-VSL		NIST		BNM-LCIE		KRISS	
Freq [GHz]	$\overline{x_u}$	$u(\overline{x_u})$	d_i	$u(d_i)$	d_i	$u(d_i)$	d_i	$u(d_i)$	d_i	$u(d_i)$	d_i	$u(d_i)$
26.5	23.422	0.127	0.041	0.133	0.022	0.408	0.058	0.136	0.062	0.259	0.068	0.233
33.0	24.387	0.135	0.056	0.140	0.077	0.410	0.163	0.143	0.267	0.184	0.123	0.348
40.0	25.100	0.234	0.056	0.237	0.040	0.424	0.030	0.238	0.680	0.651	0.014	0.604

Table 10: KCRV (unweighted mean) and degree of equivalence for the SA horn.
The uncertainty is for k=2.

Inter Laboratory Degree of Equivalence for Gain

LAB*j* →	NPL(mean)		NMi-VSL		NIST		BNM-LCIE		KRISS	
LAB*i* ↓	d_{ij}	$u(d_{ij})$	d_{ij}	$u(d_{ij})$	d_{ij}	$u(d_{ij})$	d_{ij}	$u(d_{ij})$	d_{ij}	$u(d_{ij})$
NPL(mean)			0.153	0.251	-0.017	0.040	0.353	0.147	-0.028	0.126
NMi-VSL	-0.153	0.251			-0.170	0.252	0.200	0.289	-0.181	0.279
NIST	0.017	0.040	0.170	0.252			0.370	0.149	-0.011	0.127
BNM-LCIE	-0.353	0.147	-0.200	0.289	-0.370	0.149			-0.381	0.190
KRISS	0.028	0.126	0.181	0.279	0.011	0.127	0.381	0.190		

Table 11: Degree of equivalence at 26.5 GHz for the Narda horn.
The uncertainty is for k=2.

LAB*j* →	NPL(mean)		NMi-VSL		NIST		BNM-LCIE		KRISS	
LAB*i* ↓	d_{ij}	$u(d_{ij})$	d_{ij}	$u(d_{ij})$	d_{ij}	$u(d_{ij})$	d_{ij}	$u(d_{ij})$	d_{ij}	$u(d_{ij})$
NPL(mean)			-0.043	0.251	-0.123	0.040	0.407	0.084	-0.109	0.208
NMi-VSL	0.043	0.251			-0.080	0.252	0.450	0.263	-0.066	0.324
NIST	0.123	0.040	0.080	0.252			0.530	0.086	0.014	0.208
BNM-LCIE	-0.407	0.084	-0.450	0.263	-0.530	0.086			-0.516	0.221
KRISS	0.109	0.208	0.066	0.324	-0.014	0.208	0.516	0.221		

Table 12: Degree of equivalence at 33.0 GHz for the Narda horn.
The uncertainty is for k=2.

Inter Laboratory Degree of Equivalence for Gain

LAB*j* →	NPL(mean)		NMi-VSL		NIST		BNM-LCIE		KRISS	
LAB*i* ↓	d_{ij}	$u(d_{ij})$	d_{ij}	$u(d_{ij})$	d_{ij}	$u(d_{ij})$	d_{ij}	$u(d_{ij})$	d_{ij}	$u(d_{ij})$
NPL(mean)			-0.203	0.251	-0.143	0.040	1.377	0.326	-0.074	0.395
NMi-VSL	0.203	0.251			0.060	0.252	1.580	0.410	0.129	0.467
NIST	0.143	0.040	-0.060	0.252			1.520	0.327	0.069	0.395
BNM-LCIE	-1.377	0.326	-1.580	0.410	-1.520	0.327			-1.451	0.511
KRISS	0.074	0.395	-0.129	0.467	-0.069	0.395	1.451	0.511		

Table 13: Degree of equivalence at 40.0 GHz for the Narda horn.
The uncertainty is for k=2.

LAB*j* →	NPL(mean)		NMi-VSL		NIST		BNM-LCIE		KRISS	
LAB*i* ↓	d_{ij}	$u(d_{ij})$	d_{ij}	$u(d_{ij})$	d_{ij}	$u(d_{ij})$	d_{ij}	$u(d_{ij})$	d_{ij}	$u(d_{ij})$
NPL(mean)			-0.018	0.251	-0.098	0.040	0.022	0.147	-0.108	0.128
NMi-VSL	0.018	0.251			-0.080	0.252	0.040	0.289	-0.090	0.280
NIST	0.098	0.040	0.080	0.252			0.120	0.149	-0.010	0.130
BNM-LCIE	-0.022	0.147	-0.040	0.289	-0.120	0.149			-0.130	0.192
KRISS	0.108	0.128	0.090	0.280	0.010	0.130	0.130	0.192		

Table 14: Degree of equivalence at 26.5 GHz for the SA horn.
The uncertainty is for k=2.

Inter Laboratory Degree of Equivalence for Gain

LAB*j* →	NPL(mean)		NMi-VSL		NIST		BNM-LCIE		KRISS	
LAB*i* ↓	d_{ij}	$u(d_{ij})$	d_{ij}	$u(d_{ij})$	d_{ij}	$u(d_{ij})$	d_{ij}	$u(d_{ij})$	d_{ij}	$u(d_{ij})$
NPL(mean)			0.133	0.251	-0.107	0.040	0.323	0.084	-0.067	0.209
NMi-VSL	-0.133	0.251			-0.240	0.252	0.190	0.263	-0.200	0.325
NIST	0.107	0.040	0.240	0.252			0.430	0.086	0.040	0.209
BNM-LCIE	-0.323	0.084	-0.190	0.263	-0.240	0.086			-0.390	0.222
KRISS	0.067	0.209	0.200	0.325	-0.040	0.209	0.390	0.222		

Table 15: Degree of equivalence at 33.0 GHz for the SA horn.
The uncertainty is for k=2.

LAB*j* →	NPL(mean)		NMi-VSL		NIST		BNM-LCIE		KRISS	
LAB*i* ↓	d_{ij}	$u(d_{ij})$	d_{ij}	$u(d_{ij})$	d_{ij}	$u(d_{ij})$	d_{ij}	$u(d_{ij})$	d_{ij}	$u(d_{ij})$
NPL(mean)			-0.096	0.251	-0.086	0.040	0.624	0.326	-0.042	0.395
NMi-VSL	0.096	0.251			0.010	0.252	0.720	0.410	0.054	0.467
NIST	0.086	0.040	-0.010	0.252			0.710	0.327	0.044	0.395
BNM-LCIE	-0.624	0.326	-0.720	0.410	-0.710	0.327			-0.666	0.511
KRISS	0.042	0.395	-0.054	0.467	-0.044	0.395	0.666	0.511		

Table 16: Degree of equivalence at 40.0 GHz for the SA horn.
The uncertainty is for k=2.

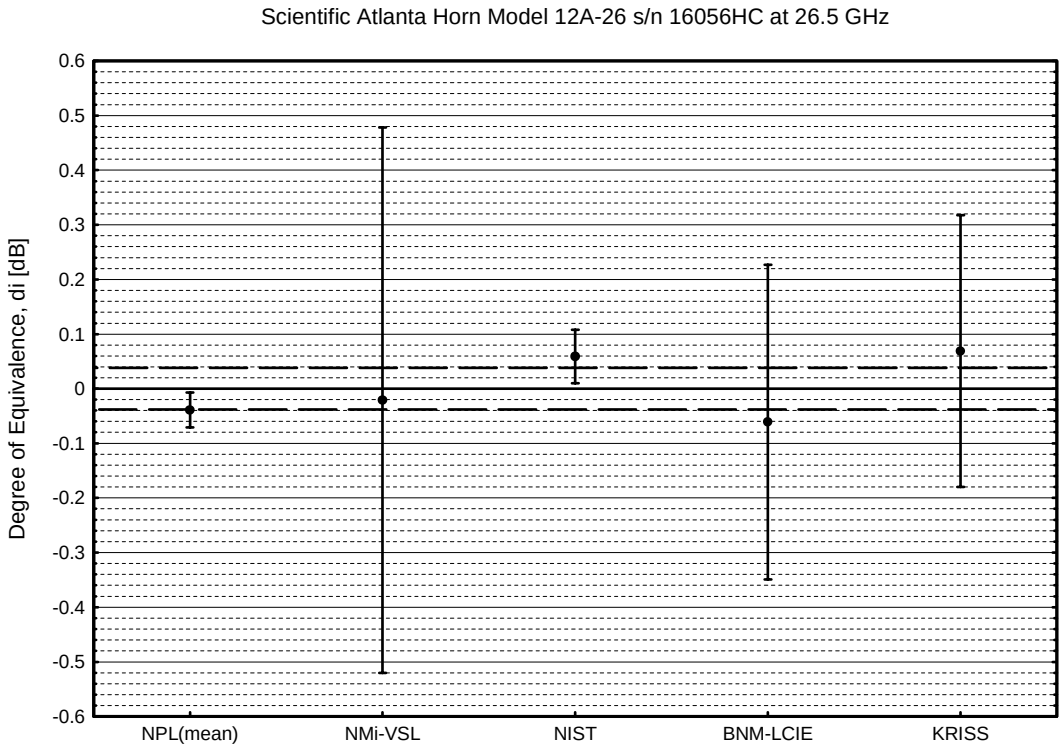

Figure 11a: Degrees of equivalence for gain for the Scientific Atlanta horn at 26.5 GHz.
The degree of equivalence with respect to the weighted mean is shown including the expanded uncertainty for k=2. The uncertainty in the weighted mean, $u(\overline{x_w})$, is shown by the dashed lines.

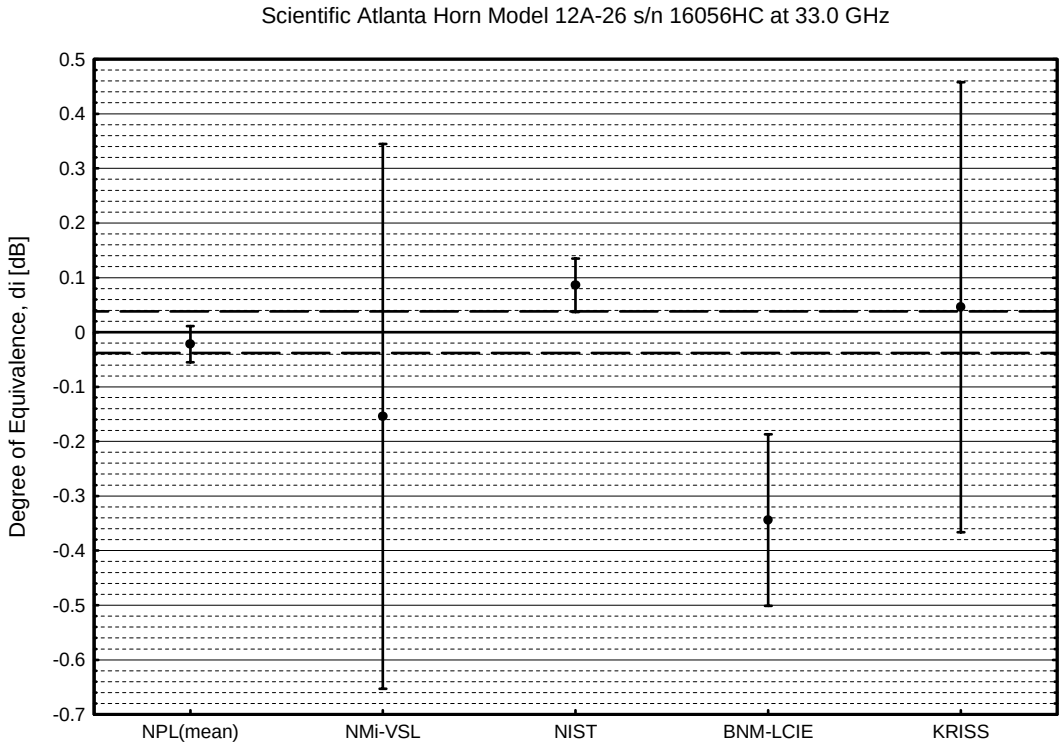

Figure 11b: Degrees of equivalence for gain for the Scientific Atlanta horn at 33.0 GHz.
The degree of equivalence with respect to the weighted mean is shown including the expanded uncertainty for k=2. The uncertainty in the weighted mean, $u(\overline{x_w})$, is shown by the dashed lines.

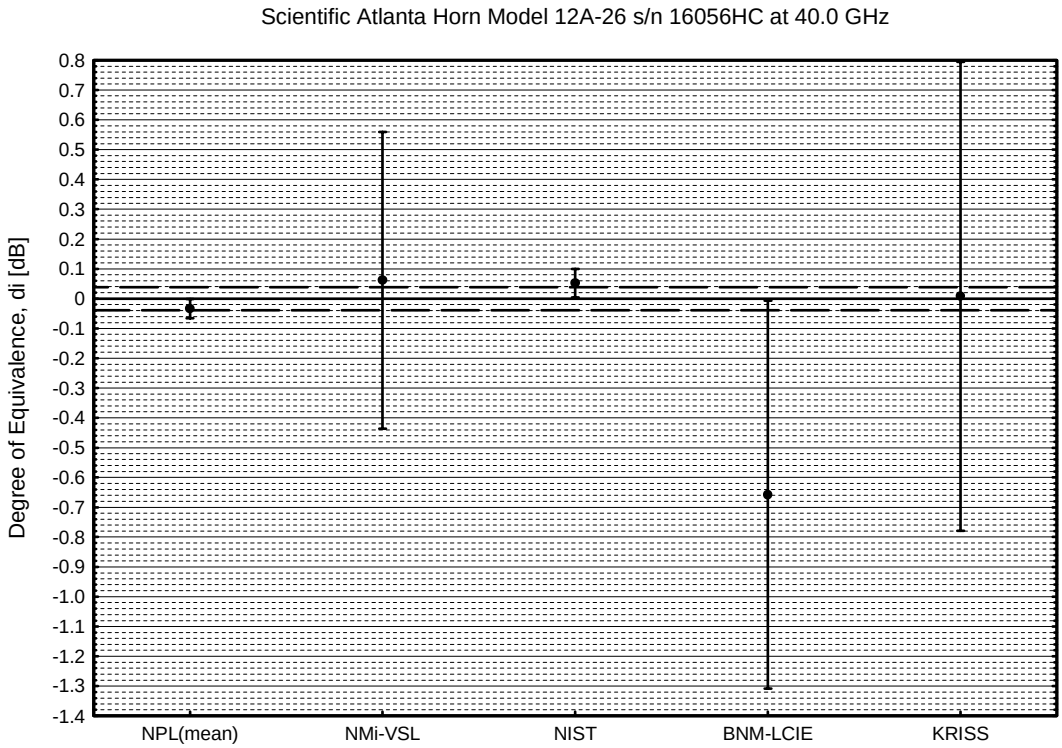

Figure 11c: Degrees of equivalence for gain for the Scientific Atlanta horn at 40.0 GHz.
The degree of equivalence with respect to the weighted mean is shown including the expanded uncertainty for k=2. The uncertainty in the weighted mean, $u(\overline{x_w})$, is shown by the dashed lines.

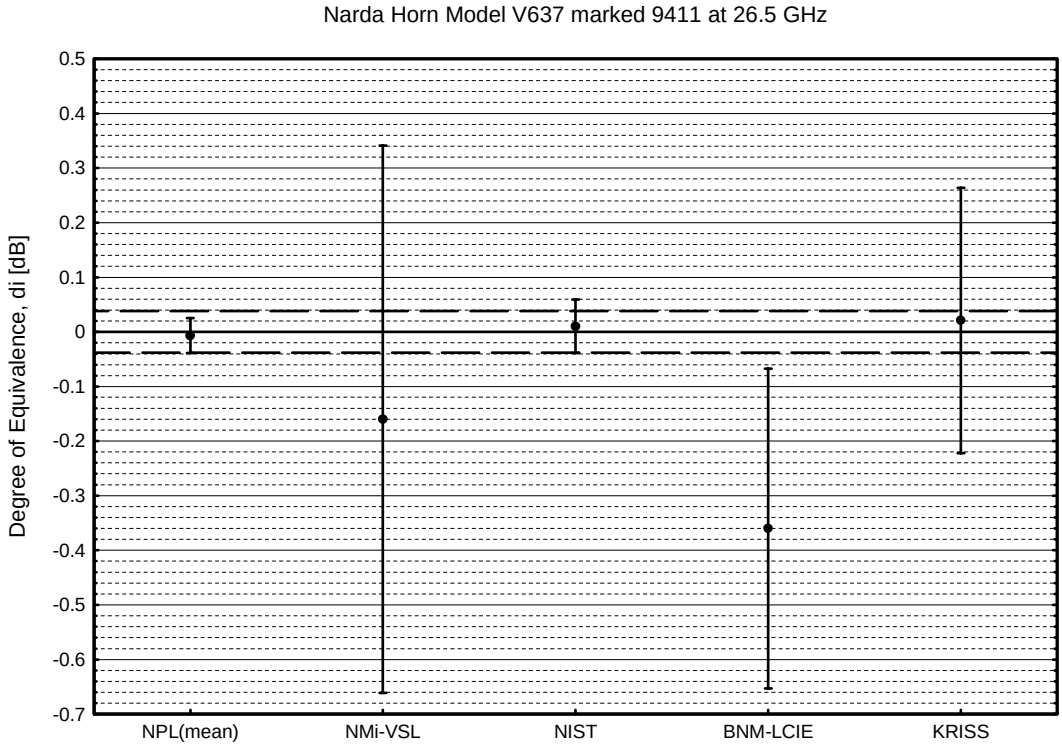

Figure 12a: Degrees of equivalence for gain for the Narda horn at 26.5 GHz.
The degree of equivalence with respect to the weighted mean is shown including the expanded uncertainty for k=2. The uncertainty in the weighted mean, $u(\overline{x_w})$, is shown by the dashed lines.

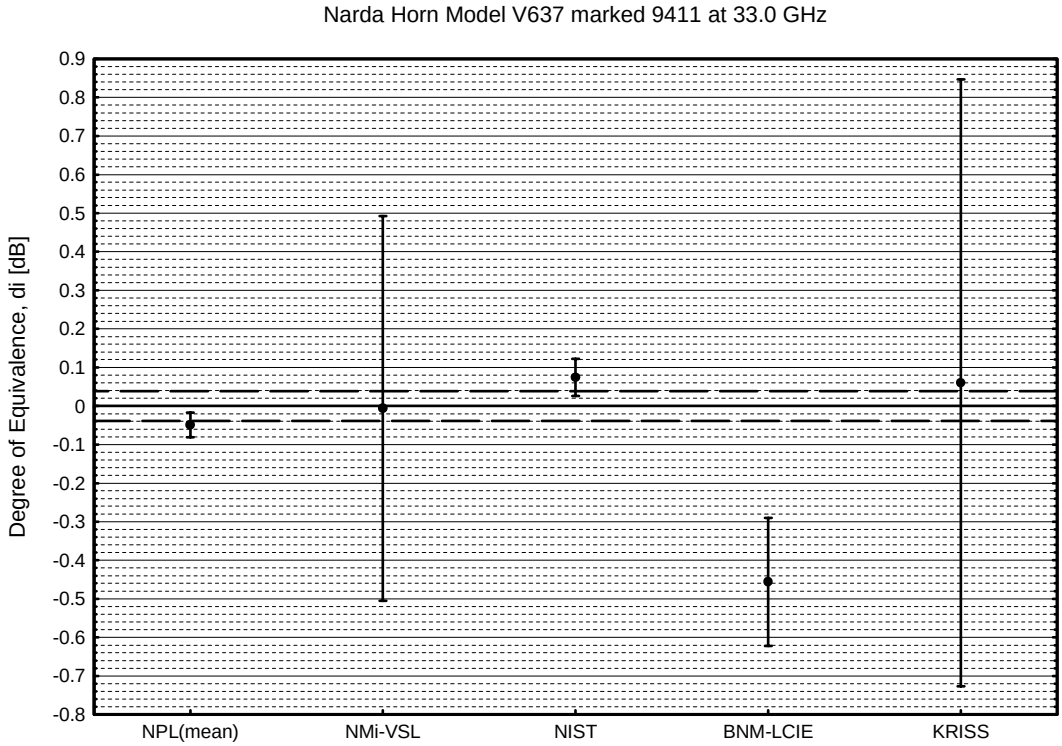

Figure 12b: Degrees of equivalence for gain for the Narda horn at 33.0 GHz.
The degree of equivalence with respect to the weighted mean is shown including the expanded uncertainty for k=2. The uncertainty in the weighted mean, $u(\overline{x_w})$, is shown by the dashed lines.

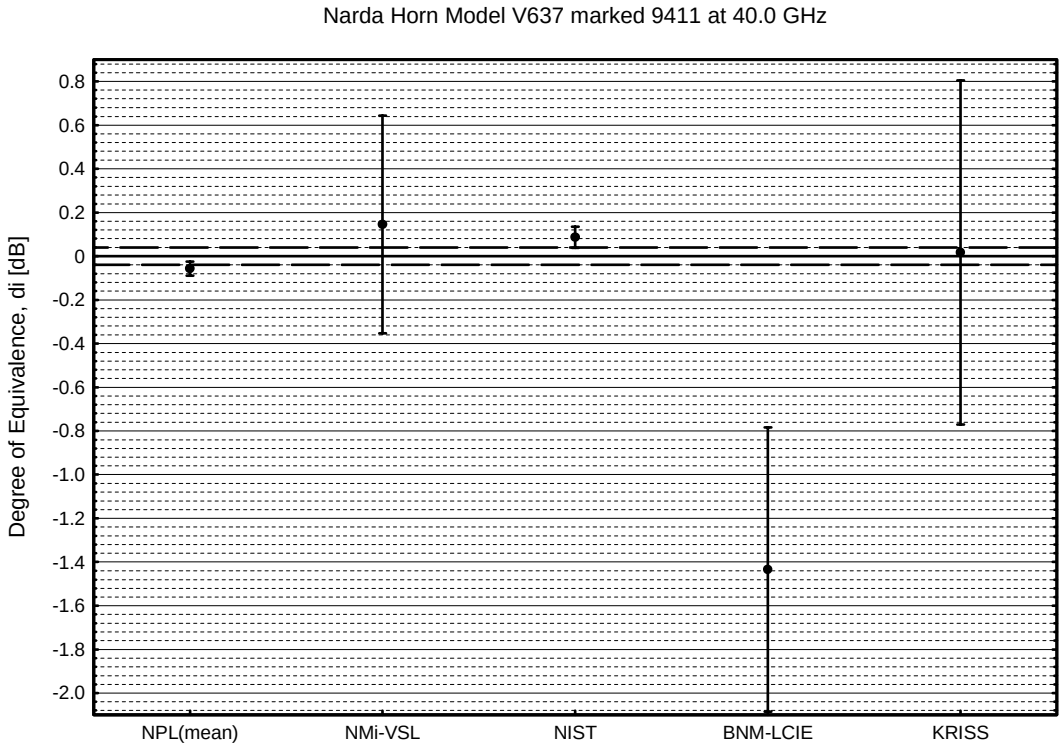

Figure 12c: Degrees of equivalence for gain for the Narda horn at 40.0 GHz.
The degree of equivalence with respect to the weighted mean is shown including the expanded uncertainty for k=2. The uncertainty in the weighted mean, $u(\overline{x_w})$, is shown by the dashed lines.

9. CONCLUSIONS

The measurement comparison has been successfully completed with a range of measurement approaches having been used by the participants. The comparison has demonstrated fairly good agreement, in the most part, between the participants. However, there are notable exceptions, and it is clear that the spread in the reported values increases markedly with frequency. Some of this increase may be explained by the fact that not all participants corrected for near zone effects, which become more significant for higher gain antennas and at higher frequencies.

There is a significant difference between the values reported by NPL and NIST for the Narda antenna at 33.0 GHz and 40.0 GHz, and for the Scientific Atlanta horn at 33.0 GHz; these are the laboratories quoting the smallest uncertainties. It would be useful for these laboratories to investigate the cause of the discrepancy as a separate exercise.

The gain value reported by BNM-LCIE at 40 GHz for the Narda antenna is significantly different from the other results, even allowing for the reported uncertainty.

Only NPL and NIST performed swept frequency gain measurements. Figure 4a and Figure 4b show that the shape of the gain versus frequency curves obtained by the two laboratories are very similar, but that there is a significant difference in the general levels of the two curves for both antennas. Also, the gain curves for the SA horn show more pronounced oscillations as a function of frequency than do the curves for the Narda horn.

The agreement between participants for the reflection coefficient measurements was very good.

The two sets of results measured by the pilot laboratory indicate that the characteristics of the travelling standards were stable throughout the duration of the exercise.

10. REFERENCES

[1] D. G. Gentle and P. R. Miller, "The Calibration of Antennas at NPL", Proceedings of the Antenna Measurement Techniques Association 21st Meeting & Symposium, Monterey, California, U.S.A., 4-8 October 1999.

[2] A.G. Repjar, A.C. Newell, and D. T. Tamura, "Extrapolation Range Measurements for Determining Antenna Gain and Polarization", NBS Technical Note 1311, August 1987.

[3] J Randa (NIST), "Proposal for KCRV & Degree of Equivalence for GT-RF Key Comparisons", GT-RF 2000/12, 8 September 2000.

[4] T.J Witt (BIPM), “Some Statistical Formulas used in the Analysis of Key Comparisons, Version 1.0”, 6 July 2001.

11. UNCERTAINTY BUDGETS

The principal components affecting the measured gain are listed in the Measurement Protocol, section 11. The tables below and their associated text give details of the uncertainty contributions for the gain for each of the participants. As the reflection coefficient measurements were considered subsidiary to the purpose of this comparison, no uncertainty budgets were requested for those measurements, only a total estimated uncertainty.

Table 17: NPL Gain Uncertainty Budget.

Symbol	Source of Uncertainty	Value +/- dB	Probability Distribution	Divisor	Ci	Ui (Kx) +/- dB	Vi or Veff
K(f) U1.1	Measurement of Transmission factor	0.0039	Normal	1	0.5000	0.002	9
K(f) U1.2	Drift of Transmission factor	0.0100	Rectangular	1.73	0.8660	0.005	Inf
U2	Repeatability of antenna connections	0.0039	Normal	1	1.2247	0.005	9
U3.1	Random error in fitting of curve	0.0020	Normal	1	0.8660	0.002	500
U3.2	Truncation of higher order terms	0.0063	Normal	1	1.1180	0.007	Inf
U3.3	Systematic fitting error	0.0020	Rectangular	1.73	1.1180	0.001	Inf
U4	Mismatch correction	0.0440	Normal	2	1.0000	0.022	Inf
U5	Cross polarisation	0.0004	Normal	2	1.0000	0.000	Inf
U6	Antenna alignment	0.0050	Normal	2	1.2247	0.003	Inf
U7	Absorber reflections	0.0079	U-shaped	1.41	1.0000	0.006	Inf
Uc(Kx)	Combined uncertainty		normal			0.025	6690
U	Expanded uncertainty		normal (k=2)			**0.050**	

Table 18: NMi-VSL Gain Uncertainty Budget.

Contributions	Value	Uncertainty	Distribution	Divisor	Standard Deviation	Subsum	Veff
Reference Power							
Reflection waveguide	0.03						
Reflection adaptor	0.075						
Reflection attenuator/detector	0.05						
Mismatch		0.0075	U-shape	√2	0.0053		∞
Uncertainty attenuator	20 dB	0.01 dB	Normal	k=1	0.0023		∞
Linearity		0.003	Rectang.	√3	0.0017		∞
Stability detection		0.001	Rectang.	√3	0.0006		∞
Subtotal						0.0061	
Transmitted Power							
Reflection waveguide	0.03						
Reflection horn 1	0.075						
Mismatch		0.0045	U-shape	√2	0.0032		∞
Reflection horn 2	0.075						
Reflection adaptor	0.075						
Reflection detector	0.05						
Mismatch		0.0188	U-shape	√2	0.0133		∞
Linearity	0.003		Rectang.	√3	0.0017		∞
Stability detection	0.001		Rectang.	√3	0.0006		∞
TOTAL 12						0.0138	
TOTAL 13		similar to TOTAL 12				0.0138	∞
TOTAL 23		similar to TOTAL 12				0.0138	∞
Distance R12	4.168m	0.004 m	Rectang.	√3		0.00055	∞
R13	4.168m	0.004 m	Rectang.	√3		0.00055	∞
R23	4.302m	0.004 m	Rectang.	√3		0.00054	∞
Frequency		1e-6	Normal	k=1	1e-6		
Scaling factor						1e-6	∞
Uncertainty in basic method		0.25 dB	Normal	k=1	0.059		
End result (linear)	256.88					15.5	∞
in dB	24.09					0.26	

Sources of Uncertainty

- *Reflection coefficients*

Instead of an absolute power measurement the “power” measured is the ratio between the power transmitted and a monitoring reading on the side arm of a directional coupler (20 dB). Hence a relatively small VSWR of the source is assumed.

For the reflection coefficients a worst case value is taken over the whole frequency range (26 – 40 GHz). In addition the combined reflections from the waveguide-coax adapter and the coaxial detector itself are summed in a similar way.

In the case of power reference measurement the mismatch uncertainty is due to interaction between the source and the adapter/detector combination.

In the case of power transmitted between the horns two terms are considered to contribute due to mismatch: on the transmitting side the interaction between source and transmitting horn, on the receiver side between the receiver horn and, on the one hand, the waveguide and, on the other hand, the adapter/detector combination.

- *Linearity and stability*

Due to the fact that at each frequency the same detectors are used only the linearity and stability of the detecting system were taken into account. In the linearity of the detector system the main contribution is due to the variation in detected power at the receiver (dependent on the frequency) and the fact that Pxy is about 20 dB lower than Pref.

- *Separation between antennas*

The determination of the separation between the two horns consists of a number of readings: it is assumed that the total uncertainty is not larger than 4 mm at 4 m separation. However, the possibility of a systematic error of 40 mm cannot be excluded (the exact location of a stop was missing in the lab notes).

- *Influence of reflections due to the absorbing material*

During all measurements the signal reflected back into the transmitting waveguide was monitored. At small distance the reflected signal was almost constant. Hence it is considered to be negligible compared to the stability and non-linearity of the detection system. In addition the effective levelling of the output using the power ratio will take care of most other contributions.

During the test phase it appeared to be necessary to add absorber material around the receiving waveguide (in the back of the receiving horn). The original ripple pattern (up to 1 dB peak-peak for the Flann/Scientific Atlanta combination at about 3 m separation) was reduced to within 0.1 dB.

As the measured gain values are within the measurement uncertainty independent of distance, it is not clear how we can estimate the contribution from reflection due to absorbers without an additional extensive measurement programme. Hence the observed variations also incorporate those contributions.

- *Signal generator and frequency*

As a source, either a synthesizer HP83640B is used (up to 21 GHz) or a HP sweeper (plug-in unit to 18.6 GHz) in combination with a frequency doubler/amplifier. The frequency stability and setting are determined by the internal ovenizer high stability reference crystal or an external synchroniser: the uncertainty of the latter (in combination with a microwave counter) is assumed to be better than 1 ppm.

- *Corrections*

No extrapolation or near-zone corrections have been applied.

- *Alignment*

Although there are in some cases significant effects due to misalignment, the positioning of the horns during the official measurements is done using fixed structures. Those structures are much better aligned than the variations used during testing.

- *Multiple reflection*

As the reflection/ripple pattern remained constant in the reflection detection system at the transmitter, a negligible multireflection between antennas is assumed at the actual measuring distance.

Basic uncertainty calculation.

As it will become clear that the uncertainty in the three antenna method is the dominating term in the total budget, only a general uncertainty budget and calculation is given and is considered to be valid for all measurements.

All sources are evaluated in a Type-B manner. The only statistically relevant parameter is the measurement result. As indicated only an estimate of the width of the distribution can be given. As the degrees of freedom are meant to estimate the need for introducing a safety term in the final uncertainty of the mean, at present there is no use for it.

Table 19: NIST Gain Uncertainty Budget.

Source of Uncertainty	Value +/- dB	Probability Distribution	Divisor	Ci	Ui (Kx) +/- dB
Receiver nonlinearity	0.0200	Rectangular	1.73	1.0000	0.012
Attenuator calibration	0.0400	Normal	3.00	1.0000	0.013
Impedance Mismatch	0.0100	Normal	3.00	1.0000	0.003
Antenna alignment	0.0300	Normal	3.00	1.0000	0.010
Distance Nonlinearity	0.0100	Normal	3.00	2.0000	0.007
Connector Loss	0.0200	Normal	3.00	1.0000	0.007
Residual multipath	0.0300	Rectangular	1.73	1.0000	0.017
Random uncertainties	0.0400	Normal	3.00	1.0000	0.013
Combined uncertainty		normal			0.031
Expanded uncertainty		normal (k=2)			**0.062**

Note: the uncertainty originally reported by NIST for all frequencies was 0.08 dB for k=3, but the uncertainty calculation did not follow the Guide to the Expression of Uncertainty in Measurement, as required in the Measurement Protocol. Table 19 was provided after the Draft A report had been circulated and NIST were asked to revise their uncertainty budget so that it conformed to the Protocol.

Table 20a: BNM-LCIE Gain Uncertainty Budget (F = 26.5 GHz)

Source of uncertainty	Value ± (dB)	Probability distribution	Divisor	Standard deviation
Signal generator and frequency	0.00041	Rectangular	1.73	0.00024
Antenna positioning and displacement	0.00639	Rectangular	1.73	0.00369
Impedance mismatch	0.01209	U-shape	1.41	0.00855
Free space area and absorbing material	0.00124	U-shape	1.41	0.00088
Measurement repeatability	0.14500	Normal	1	0.14500
Combined uncertainty		Normal		0.14530
Expanded uncertainty		Normal (k=2)		0.29

Note: the uncertainty originally reported by BNM-LCIE for all frequencies was 0.36 dB for k=1, but the uncertainty calculation did not follow the Guide to the Expression of Uncertainty in Measurement, as required in the Measurement Protocol. Tables 20a, 20b and 20c were provided after the Draft A report had been circulated and BNM-LCIE were asked to revise their uncertainty budget so that it conformed to the Protocol.

Table 20b: BNM-LCIE Gain Uncertainty Budget (F = 33 GHz)

Source of uncertainty	Value ± (dB)	Probability distribution	Divisor	Standard deviation
Signal generator and frequency	0.00046	Rectangular	1.73	0.00027
Antenna positioning and displacement	0.00664	Rectangular	1.73	0.00384
Impedance mismatch	0.01148	U-shape	1.41	0.00812
Free space area and absorbing material	0.00126	U-shape	1.41	0.00089
Measurement repeatability	0.08000	Normal	1	0.08000
Combined uncertainty		Normal		0.08051
Expanded uncertainty		Normal (k=2)		0.16

Table 20c: BNM-LCIE Gain Uncertainty Budget (F = 40 GHz)

Source of uncertainty	Value ± (dB)	Probability distribution	Divisor	Standard deviation
Signal generator and frequency	0.00010	Rectangular	1.73	0.00006
Antenna positioning and displacement	0.00149	Rectangular	1.73	0.00086
Impedance mismatch	0.01069	U-shape	1.41	0.00756
Free space area and absorbing material	0.00749	U-shape	1.41	0.00530
Measurement repeatability	0.32500	Normal	1	0.32500
Combined uncertainty		Normal		0.32513
Expanded uncertainty		Normal (k=2)		0.65

The different contributions in the calculation of the uncertainty budget are related to:

- The signal generator and frequency taking into account the uncertainty on the frequency itself generated by the synthesizer. It is the lowest term in the uncertainty budget whatever the frequency of operation.
- The positioning and the free space between antennas taking into account the uncertainty on the displacement of antennas.
- The impedance mismatch taking into account the uncertainty on the reflection coefficient present at the input of the antennas. It is one of the important terms in the uncertainty budget.
- The free space area including the absorbing materials and taking into account the uncertainty on the attenuation of the free site between antennas.
- The measurement repeatability by connecting and disconnecting the antennas under test. The number of connections was only two connections. It clearly appears that this contribution has the highest term in the uncertainty budget. More investigations are needed in the future in order to improve our measurement technique.

Table 21a: KRISS Gain Uncertainty Budget for SA horn 12A-26, marked "INT" at 26.5 GHz

Standard Uncertainty Component $u(x_i)$	Source of Uncertainty	Value of Standard Uncertainty $u(x_i)$	$c_i = \partial f / \partial x_i$	$c_i u(x_i)$	Degrees Of Freedom
$u(R_{12})$	Square root of the Gain product for antenna pair 1	0.070 dB	1	0.070 dB	45
$u(R_{13})$	Square root of the Gain product for antenna pair 2	0.069 dB	1	0.069 dB	43
$u(R_{23})$	Square root of the Gain product for antenna pair 3	0.073 dB	1	0.073 dB	54
$u(R_1)$	Direct connection measurement	0.009 dB	1	0.009 dB	59
$u(R_2)$	System drift	0.003 dB	1	0.003 dB	∞
$u(R_3)$	Extrapolation	0.010 dB	1	0.010 dB	11
$u(R_4)$	Antenna alignment	0.044 dB	1	0.044 dB	∞
$u(R_5)$	Multiple reflections between antennas	0.003 dB	1	0.003 dB	∞
$u(R_6)$	Reflection from RAM	0.014 dB	1	0.014 dB	∞
$u(R_7)$	Receiver linearity	0.049 dB	1	0.049 dB	11
$u(M_1)$	Mismatch correction factor	0.021 dB	1	0.029 dB	1481
$u(\lvert\Gamma_1\rvert)$	Magnitude of reflection coefficient of antenna 1	0.004	0.234	$1.4\text{x}10^{-3}$	11
$u(\lvert\Gamma_2\rvert)$	Magnitude of reflection coefficient of antenna 2	0.004	0.012	$7.2\text{x}10^{-5}$	11
$u(\lvert\Gamma_G\rvert)$	Magnitude of reflection coefficient of transmitter	0.004	0.138	$8.3\text{x}10^{-4}$	11
$u(\lvert\Gamma_L\rvert)$	Magnitude of reflection coefficient of receiver	0.004	0.005	$3.0\text{x}10^{-5}$	11
$u(\phi_1)$	Phase of reflection coefficient of antenna 1	0.104 rad	-0.011	$-1.5\text{x}10^{-3}$	11
$u(\phi_2)$	Phase of reflection coefficient of antenna 2	0.144 rad	0.001	$2.0\text{x}10^{-4}$	11
$u(\phi_G)$	Phase of reflection coefficient of transmitter	0.087 rad	-0.015	$-1.5\text{x}10^{-3}$	11
$u(\phi_L)$	Phase of reflection coefficient of receiver	0.097 rad	-0.007	$-8.5\text{x}10^{-4}$	11
$u(G_1)$	Gain of antenna 1	0.125 dB			158

Table 21b: KRISS Gain Uncertainty Budget for SA horn 12A-26, marked "INT" at 33 GHz

Standard Uncertainty Component $u(x_i)$	Source of Uncertainty	Value of Standard Uncertainty $u(x_i)$	$c_i = \partial f / \partial x_i$	$c_i u(x_i)$	Degrees Of Freedom
$u(R_{12})$	Square root of the Gain product for antenna pair 1	0.119 dB	1	0.119 dB	16
$u(R_{13})$	Square root of the Gain product for antenna pair 2	0.119 dB	1	0.119 dB	16
$u(R_{23})$	Square root of the Gain product for antenna pair 3	0.119 dB	1	0.119 dB	16
$u(R_1)$	Direct connection measurement	0.006 dB	1	0.006 dB	12
$u(R_2)$	System drift	0.002 dB	1	0.002 dB	∞
$u(R_3)$	Extrapolation	0.011 dB	1	0.011 dB	11
$u(R_4)$	Antenna alignment	0.044 dB	1	0.044 dB	∞
$u(R_5)$	Multiple reflections between antennas	0.001 dB	1	0.001 dB	∞
$u(R_6)$	Reflection from RAM	0.014 dB	1	0.014 dB	∞
$u(R_7)$	Receiver linearity	0.108 dB	1	0.108 dB	11
$u(M_1)$	Mismatch correction factor	0.015 dB	1	0.017 dB	1162
$u(\lvert\Gamma_1\rvert)$	Magnitude of reflection coefficient of antenna 1	0.004	-0.122	$-7.3\text{x}10^{-4}$	11
$u(\lvert\Gamma_2\rvert)$	Magnitude of reflection coefficient of antenna 2	0.004	0.164	$9.8\text{x}10^{-4}$	11
$u(\lvert\Gamma_G\rvert)$	Magnitude of reflection coefficient of transmitter	0.004	-0.087	$-5.2\text{x}10^{-4}$	11
$u(\lvert\Gamma_L\rvert)$	Magnitude of reflection coefficient of receiver	0.004	-0.082	$-4.9\text{x}10^{-4}$	11
$u(\phi_1)$	Phase of reflection coefficient of antenna 1	0.144 rad	0.005	$9.7\text{x}10^{-4}$	11
$u(\phi_2)$	Phase of reflection coefficient of antenna 2	0.190 rad	0.0006	$1.6\text{x}10^{-4}$	11
$u(\phi_G)$	Phase of reflection coefficient of transmitter	0.080 rad	0.002	$1.9\text{x}10^{-4}$	11
$u(\phi_L)$	Phase of reflection coefficient of receiver	0.118 rad	-0.002	$-3.1\text{x}10^{-4}$	11
$u(G_1)$	Gain of antenna 1	0.207 dB			49

Table 21c: KRISS Gain Uncertainty Budget for SA horn 12A-26, marked "INT" at 40 GHz

Standard Uncertainty Component $u(x_i)$	Source of Uncertainty	Value of Standard Uncertainty $u(x_i)$	$c_i = \partial f / \partial x_i$	$c_i u(x_i)$	Degrees Of Freedom
$u(R_{12})$	Square root of the Gain product for antenna pair 1	0.227 dB	1	0.227 dB	12
$u(R_{13})$	Square root of the Gain product for antenna pair 2	0.227 dB	1	0.227 dB	12
$u(R_{23})$	Square root of the Gain product for antenna pair 3	0.227 dB	1	0.227 dB	12
$u(R_1)$	Direct connection measurement	0.020 dB	1	0.020 dB	784
$u(R_2)$	System drift	0.005 dB	1	0.005 dB	∞
$u(R_3)$	Extrapolation	0.011 dB	1	0.011 dB	11
$u(R_4)$	Antenna alignment	0.044 dB	1	0.044 dB	∞
$u(R_5)$	Multiple reflections between antennas	0.003 dB	1	0.003 dB	∞
$u(R_6)$	Reflection from RAM	0.014 dB	1	0.014 dB	∞
$u(R_7)$	Receiver linearity	0.222 dB	1	0.222 dB	11
$u(M_1)$	Mismatch correction factor	0.010 dB	1	0.015 dB	528
$u(\lvert\Gamma_1\rvert)$	Magnitude of reflection coefficient of antenna 1	0.004	0.215	$1.3\text{x}10^{-3}$	11
$u(\lvert\Gamma_2\rvert)$	Magnitude of reflection coefficient of antenna 2	0.004	0.019	$1.1\text{x}10^{-4}$	11
$u(\lvert\Gamma_G\rvert)$	Magnitude of reflection coefficient of transmitter	0.004	0.086	$5.2\text{x}10^{-4}$	11
$u(\lvert\Gamma_L\rvert)$	Magnitude of reflection coefficient of receiver	0.004	0.011	$6.6\text{x}10^{-5}$	11
$u(\phi_1)$	Phase of reflection coefficient of antenna 1	0.164 rad	0.001	$2.2\text{x}10^{-4}$	11
$u(\phi_2)$	Phase of reflection coefficient of antenna 2	0.288 rad	-0.001	$-4.5\text{x}10^{-4}$	11
$u(\phi_G)$	Phase of reflection coefficient of transmitter	0.010 rad	0.001	$1.3\text{x}10^{-4}$	11
$u(\phi_L)$	Phase of reflection coefficient of receiver	0.231 rad	0.001	$3.4\text{x}10^{-4}$	11
$u(G_1)$	Gain of antenna 1	0.394 dB			36

Table 21d: KRISS Gain Uncertainty Budget for Narda V637, marked "INT" at 26.5 GHz

Standard Uncertainty Component $u(x_i)$	Source of Uncertainty	Value of Standard Uncertainty $u(x_i)$	$c_i = \partial f / \partial x_i$	$c_i u(x_i)$	Degrees Of Freedom
$u(R_{12})$	Square root of the Gain product for antenna pair 1	0.070 dB	1	0.070 dB	45
$u(R_{13})$	Square root of the Gain product for antenna pair 2	0.069 dB	1	0.069 dB	43
$u(R_{23})$	Square root of the Gain product for antenna pair 3	0.073 dB	1	0.073 dB	54
$u(R_1)$	Direct connection measurement	0.009 dB	1	0.009 dB	59
$u(R_2)$	System drift	0.003 dB	1	0.003 dB	∞
$u(R_3)$	Extrapolation	0.010 dB	1	0.010 dB	11
$u(R_4)$	Antenna alignment	0.044 dB	1	0.044 dB	∞
$u(R_5)$	Multiple reflections between antennas	0.003 dB	1	0.003 dB	∞
$u(R_6)$	Reflection from RAM	0.014 dB	1	0.014 dB	∞
$u(R_7)$	Receiver linearity	0.049 dB	1	0.049 dB	11
$u(M_2)$	Mismatch correction factor	0.011 dB	1	0.013 dB	793
$u(\lvert\Gamma_2\rvert)$	Magnitude of reflection coefficient of antenna 2	0.004	-0.082	$-5.0\text{x}10^{-4}$	11
$u(\lvert\Gamma_G\rvert)$	Magnitude of reflection coefficient of transmitter	0.004	-0.001	$-6.0\text{x}10^{-6}$	11
$u(\lvert\Gamma_L\rvert)$	Magnitude of reflection coefficient of receiver	0.004	0.005	$3.0\text{x}10^{-5}$	11
$u(\phi_2)$	Phase of reflection coefficient of antenna 2	0.144 rad	-0.002	$-4.0\text{x}10^{-4}$	11
$u(\phi_G)$	Phase of reflection coefficient of transmitter	0.087 rad	-0.008	$-8.4\text{x}10^{-3}$	11
$u(\phi_L)$	Phase of reflection coefficient of receiver	0.097 rad	-0.007	$-8.5\text{x}10^{-3}$	11
$u(G_2)$	Gain of antenna 2	0.123 dB			144

Table 21e: KRISS Gain Uncertainty Budget for Narda V637, marked "INT" at 33 GHz

Standard Uncertainty Component $u(x_i)$	Source of Uncertainty	Value of Standard Uncertainty $u(x_i)$	$c_i = \partial f / \partial x_i$	$c_i u(x_i)$	Degrees Of Freedom
$u(R_{12})$	Square root of the Gain product for antenna pair 1	0.119 dB	1	0.119 dB	16
$u(R_{13})$	Square root of the Gain product for antenna pair 2	0.119 dB	1	0.119 dB	16
$u(R_{23})$	Square root of the Gain product for antenna pair 3	0.119 dB	1	0.119 dB	16
$u(R_1)$	Direct connection measurement	0.006 dB	1	0.006 dB	12
$u(R_2)$	System drift	0.002 dB	1	0.002 dB	∞
$u(R_3)$	Extrapolation	0.011 dB	1	0.011 dB	11
$u(R_4)$	Antenna alignment	0.044 dB	1	0.044 dB	∞
$u(R_5)$	Multiple reflections between antennas	0.001 dB	1	0.001 dB	∞
$u(R_6)$	Reflection from RAM	0.014 dB	1	0.014 dB	∞
$u(R_7)$	Receiver linearity	0.108 dB	1	0.108 dB	11
$u(M_2)$	Mismatch correction factor	0.005 dB	1	0.008 dB	1071
$u(\lvert\Gamma_2\rvert)$	Magnitude of reflection coefficient of antenna 2	0.004	-0.016	-9.6×10^{-5}	11
$u(\lvert\Gamma_G\rvert)$	Magnitude of reflection coefficient of transmitter	0.004	-0.072	-4.3×10^{-4}	11
$u(\lvert\Gamma_L\rvert)$	Magnitude of reflection coefficient of receiver	0.004	-0.082	-4.9×10^{-4}	11
$u(\phi_2)$	Phase of reflection coefficient of antenna 2	0.190 rad	0.001	2.7×10^{-4}	11
$u(\phi_G)$	Phase of reflection coefficient of transmitter	0.080 rad	-0.002	-1.9×10^{-4}	11
$u(\phi_L)$	Phase of reflection coefficient of receiver	0.118 rad	-0.002	-3.1×10^{-4}	11
$u(G_2)$	Gain of antenna 2	0.206 dB			48

Table 21f: KRISS Gain Uncertainty Budget for Narda V637, marked "INT" at 40 GHz

Standard Uncertainty Component $u(x_i)$	Source of Uncertainty	Value of Standard Uncertainty $u(x_i)$	$c_i = \partial f / \partial x_i$	$c_i u(x_i)$	Degrees Of Freedom
$u(R_{12})$	Square root of the Gain product for antenna pair 1	0.227 dB	1	0.227 dB	12
$u(R_{13})$	Square root of the Gain product for antenna pair 2	0.227 dB	1	0.227 dB	12
$u(R_{23})$	Square root of the Gain product for antenna pair 3	0.227 dB	1	0.227 dB	12
$u(R_1)$	Direct connection measurement	0.020 dB	1	0.020 dB	784
$u(R_2)$	System drift	0.005 dB	1	0.005 dB	∞
$u(R_3)$	Extrapolation	0.011 dB	1	0.011 dB	11
$u(R_4)$	Antenna alignment	0.044 dB	1	0.044 dB	∞
$u(R_5)$	Multiple reflections between antennas	0.003 dB	1	0.003 dB	∞
$u(R_6)$	Reflection from RAM	0.014 dB	1	0.014 dB	∞
$u(R_7)$	Receiver linearity	0.222 dB	1	0.222 dB	11
$u(M_2)$	Mismatch correction factor	0.005 dB	1	0.008 dB	1967
$u(\lvert\Gamma_2\rvert)$	Magnitude of reflection coefficient of antenna 2	0.004	-0.024	$-1.4\text{x}10^{-4}$	11
$u(\lvert\Gamma_G\rvert)$	Magnitude of reflection coefficient of transmitter	0.004	-0.001	$-6.0\text{x}10^{-6}$	11
$u(\lvert\Gamma_L\rvert)$	Magnitude of reflection coefficient of receiver	0.004	0.011	$6.6\text{x}10^{-5}$	11
$u(\phi_2)$	Phase of reflection coefficient of antenna 2	0.288 rad	0.001	$4.5\text{x}10^{-4}$	11
$u(\phi_G)$	Phase of reflection coefficient of transmitter	0.010 rad	0.002	$2.5\text{x}10^{-4}$	11
$u(\phi_L)$	Phase of reflection coefficient of receiver	0.231 rad	0.001	$3.4\text{x}10^{-4}$	11
$u(G_2)$	Gain of antenna 2	0.394 dB			36

12. ACKNOWLEDGEMENTS

The authors would like to acknowledge the valuable assistance of Dr Ulrich Stumper of PTB, Germany and his colleagues Dr Thorsten Schrader and Klaus Muenter who read through the draft B report of the intercomparison and provided many useful comments and checked the calculations.

The work of the pilot laboratory was undertaken within the Electrical Programme of the DTI's National Measurement System Policy Unit.